2011 年臺灣國際科學展覽會

優勝作品專輯

編號：030002

作品名稱

Emitting Gold Nanodots Synthesized via Protein Templates

得獎獎項

一等獎

美國正選代表:美國第 62 屆國際科技展覽會

作者姓名：簡韻真

就讀學校：臺北市立第一女子高級中學

指導教師：周必泰、詹莉芬

關鍵字：胰島素、金奈米粒子、螢光

作者簡介

　　我是來自北一女中的簡韻真，一路誤打誤撞的跑進複選，即使之前是因學姐的熱情所以投身實驗。在實驗室的時光很歡樂也辛苦，驚恐的發現自己運動量急速下降，更發現做越多，越知道自己書讀得不夠。最要感謝的是一路上有朋友、師長相陪。謝謝你們！

Emitting Gold Nanodots Synthesized via Protein Templates

蛋白質輔助發光金奈米粒子合成之研究

摘要

本研究利用蛋白質的環保、生物活性，金奈米粒子的低毒性，及蛋白質金奈米粒子的螢光特性，合成可應用於生物體內之螢光蛋白質金奈米粒子，從而利於標靶藥物研究。本研究選擇與眾多疾病相關的胰島素，以最佳方式合成紅色螢光胰島素金奈米粒子，有助於探討糖尿病相關機制。並嘗試以養晶得到結晶狀的胰島素金奈米粒子；經由離子測試發現胰島素金奈米粒子十分穩定，更可應用於細胞內微量氰離子檢測；根據 CD 光譜，確認胰島素金奈米粒子與胰島素的蛋白質二級結構相似。之後利用 MTT 測試細胞毒性，並將胰島素金奈米粒子餵入細胞，並取得細胞螢光影像，證明胰島素金奈米粒子可經由細胞表面之胰島素受體進入細胞內，且呈現紅色螢光，證明胰島素金奈米粒子可用於生物體內顯影追蹤。利用老鼠實驗證明胰島素金奈米粒子具有胰島素降血糖之功用。

Abstract

Fluorescent nanomaterials have shown great promise for applications such as sensing, imaging and light emitting devices. Most of the nanoclusters, however, are toxic in vivo. Gold nanodots are least biologically toxic among them. To synthesize gold nanodots with disease-related protein, such as insulin can help scientists to learn more about the mechanism of diabetes and Alzheimer by tracing the fluorescent insulin gold nanodots(insulin-Au NDs) in vivo.

The fluorescence of the insulin-Au NDs is affected by pH value, reaction time, temperature, gold ion concentration and the buffer. The insulin-Au NDs crystals are made by soaking insulin crystals into $HAuCl_{4(aq)}$ solution, which may be helpful to defining the structure of protein-Au NDs. According to the Stern-Volmer plot of fluorescence quenching of the Au NCs by cyanide, protein-Au NDs can be cyanide ion detector in solution even in vivo. The insulin-Au NDs have been successfully fed into cells through insulin receptors on cell membrane, which preliminarily confirms the biological activity of insulin-Au NDs.The result of the MTT assay shows that the cytotoxicity of insulin-Au NDs is really low, so it is safer to trace insulin in vivo by insulin-Au NDs' fluorescence instead of radiolabeling. In insulin tolerance test, Human-Regular insulin and insulin-Au NDs show the same capability to lower the blood sugar concentration of mice, which means the biological activity of insulin Au@NDs is similar to insulin.

目錄

表目錄

圖目錄

壹、 前言

一、研究動機與文獻探討

近年來，奈米科技蓬勃發展，廣泛應用於材料、化學、生物等諸多領域。其中，目前雖有眾多的材料應用在生物領域，例如利用銀奈米粒子殺菌，但其對一般正常活體亦具有相當的毒性，如果想要在生物活體上應用，目前金奈米粒子仍是公認最不具生物毒性的奈米材料。

當金奈米粒子小於 2 nm 時，視所接的配位基，會發出螢光。文獻指出在鹼性環境下，使用牛血清白蛋白（BSA）還原金離子，其所產生的紅色螢光 BSA@Au，具備高穩定性、低毒性且有生物活性的優點。亦可被用來偵測水溶液中氰離子與汞離子的濃度。

本研究初步目標為改善牛血清白蛋白金奈米粒子(BSA@Au)的發光效率(Q.Y.)。更進一步，製作出其他螢光蛋白質金奈米，使之可以因其螢光，具體應用於生物活體上。例如使用與糖尿病、阿茲海默症、肥胖等疾病相關的胰島素，合成螢光胰島素金奈米粒子，以利探討這些疾病之相關機制。

二、研究目的

(一) 以還原劑增進 BSA@Au 的發螢光效率。

(二) 使用其他蛋白質製作蛋白質金奈米粒子，例如嘗試可殺菌的溶菌酶、與糖尿病密切相關的胰島素等等。

(三) 找尋製作胰島素金奈米粒子之最佳流程，並確認其形態。

(四) 找尋胰島素金奈米粒子之化學應用。

(五) 證明胰島素金奈米粒子具有生物活性。

貳、 研究方法與過程

一、 研究設備與器材

(一) 實驗器材

表 1 實驗器材

項目	規格	數量
電子天平	小數下四位	1 台
超音波震盪器		1 台
結晶盒	24 洞/96 洞	10 盒
Microtube	Appendorf	數個
樣品瓶	7mL、20mL	數個
自動滴管	2μL、10μL、20μL、200μL、1 mL、5 mL	各一支
電泳槽		1 個
離心機		1 台
磁石攪拌加熱器		1 台
光學石英瓶		2 個
Millipore	<1nm	數個

(二) 實驗藥品

表 2 實驗藥品

試藥	英文名稱	分子量	廠牌	純度
$HAuCl_4$	Gold(Ⅲ) Chloride	303.32	ACROS CHIMCA N.V	99%
NaOH	Sodium Hydroxide	40.00	Shimakyu's Pure Chemicals	>98%
TBAB	Tetrabutylammonium Bromide	322.37	東京化成工業株式會社	>99%
Na_2HPO_4	Disodium hydrogen phosphate	141.96	SIGMA-ALDRICH	>98.5%
Na_3PO_4	Sodium phosphate	163.94	ALDRICH	96%

BSA	Albumin Bovine	66kDa	SIGMA-ALDRICH	>96%
LGRM	L-Glutathione reduced	307.32	SIGMA-ALDRICH	>99%
HB	Hemoglobin Human		SIGMA-ALDRICH	
MB	Myoglobin, from canine heart	16.7kDa	SIGMA-ALDRICH	>95%
Insulin	Insulin, from bivine pancreas,I6634	5.8KDa	SIGMA-ALDRICH	
Lysozyme	Lysozyme Chloride, from chicken egg white	14.7kDa	SIGMA-ALDRICH	>90%
C480	2,3,6,7-tetrahydro-9-methyl -1H,5H,11H-[1]benzopyrano- [6,7,8-ij] quinolizin-11-one; Coumain 102	255.32	Exciton	
DCM	4-dicyanomethylene-2-methyl-6-p-dimethylaminostyryl-4H-pyran	303.35	Exciton	
NaCN	Sodium cyanide		Sigma	
Humulin-regular			Eli Lilly	

(三) 實驗儀器

1. Firstek(S 300R) orbital shaking incubator

2. Hitachi(U-3310) spectrophotometer

3. Edinburgh(FS920) fluorimeter

4. FLIM(Fluorescent Lifetime Imaging Microscopy)

5. Jasco(J-810) spectropolarmeter

二、增進 BSA@Au 發螢光效率

先依照文獻作法製作 BSA@Au：配 50 mg/mL BSA$_{(aq)}$ 5 mL，在 37℃ 下加入 20 mg/mL HAuCl$_{4(aq)}$ 1 mL、1 M NaOH$_{(aq)}$ 1 mL 以提供鹼性環境，持續攪拌 12 小時。接著改變反應中 BSA$_{(aq)}$ 的濃度、反應時間及加入還原劑。以 UV 光照射樣品檢驗螢光，再測其吸收與螢光光譜。

三、引入不同蛋白質

(一) 血清蛋白

首先嘗試與 BSA 同為血清蛋白的蛋白質，來製作其他種類之蛋白質金奈米粒子。先取 LGRM$_{(aq)}$ 100 mg，溶於 1 mL 的去離子水中，加入 1 M NaOH$_{(aq)}$ 1 mL，使用 0.1 M TBAB$_{(aq)}$ 1 mL 作為還原劑，最後加入 20 mg/mL HAuCl$_{4(aq)}$ 1 mL，使總體積為 4 mL。

重複上述實驗步驟，將 LGRM$_{(aq)}$ 更改為 HB$_{(aq)}$、MB$_{(aq)}$，並調整 NaOH$_{(aq)}$ 濃度、蛋白質濃度、TBAB$_{(aq)}$ 濃度作為變因，照射 UV 光以檢驗樣品是否會有螢光。

(二) 溶菌酶與胰島素

為了使反應條件單純，使用易結晶之蛋白質合成蛋白質金奈米粒子，以俾結晶純化。因此選用易結晶且生物應用性高的溶菌酶(lysozyme)與胰島素(insulin)。

1. 製作溶菌酶金奈米粒子

將溶菌酶 5 mg 溶於 1 mL 去離子水中，加入 1 M NaOH$_{(aq)}$ 0.25 mL、20 mg/mL HAuCl$_{4\,(aq)}$ 1 mL，持續攪拌三小時。重複上述步驟，改變溶菌酶濃度、NaOH$_{(aq)}$ 濃度、HAuCl$_{4(aq)}$ 濃度，加入還原劑 TBAB$_{(aq)}$、5% NaCl$_{(aq)}$，之

後觀察照 UV 光結果，以挑選發光效果較佳之樣品。測其吸收與螢光光譜後，以染料 C480 作為基準，計算 Q.Y.。

測溶菌酶金奈米粒子之 SDS 膠體電泳，以觀察其分子大小是否適宜結晶。

2. 製作胰島素金奈米粒子

將胰島素 7.3 mg 溶於 1.85 mL 的去離子水中，1 M $NaOH_{(aq)}$ 0.1 mL、20 mg/mL $HAuCl_4$ $_{(aq)}$ 0.05 mL，持續攪拌四小時。重複上述步驟，更換不同濃度的胰島素與 $HAuCl_4$ $_{(aq)}$，且溶於緩衝溶液，或調整 $NaOH_{(aq)}$濃度。觀察樣品照 UV 光的結果，從中挑選發光效果較佳之樣品測光譜，以染料 C480 作為基準，計算其 Q.Y.。

測胰島素金奈米粒子之 SDS 膠體電泳，以觀察其分子大小是否適宜結晶。

四、改善與測定胰島素金奈米粒子

(一) 胰島素金奈米粒子結晶

參考文獻中蛋白質與金屬離子結晶的實驗，先製作胰島素晶體，再將胰島素晶體撈出，泡入含有金離子的溶液中。

依照文獻做法配置 reservoir：將 0.5 M Na_2HPO_4 $_{(aq)}$ 5.25 mL、0.5 M, Na_3PO_4 $_{(aq)}$ 1.75 mL 與去離子水 3 mL 混合，做為最高濃度。重複上述步驟，更改 0.5 M Na_2HPO_4 $_{(aq)}$ 5.25 mL 與 0.5 M, Na_3PO_4 $_{(aq)}$ 與去離子水的比例，總體積皆為 10 mL。

使用 96 洞的結晶盤，在每一槽中間置放 200 μL reservoir；24 洞結晶盤，在每一槽中間置放 500 μL reservoir。為了找出最佳結晶條件，改變 reservoir 濃度、胰島素濃度、reservoir 與胰島素的比例(2 μL＋2 μL)、(3 μL＋1 μL)，觀察並記錄各槽結晶狀況，選定最佳結晶條件。

選取完整的胰島素結晶放入 HAuCl$_4$ $_{(aq)}$中，使金離子進入胰島素晶體，觀察晶體結構變化，並檢測胰島素晶體放入 HAuCl$_4$ $_{(aq)}$溶液前後之吸收與螢光光譜。

(二) 提高胰島素金奈米粒子發光效率

1. 改變溫度

反覆調整不同反應物濃度後，因有文獻將蛋白質金奈米粒子加熱，以提高其發光效率，本實驗將胰島素金奈米粒子置於高溫下，同時另一組在低溫下製作。

取胰島素 10 mg，溶於鹼性緩衝溶液 800 μL，迅速加入 20 mg/mL HAuCl$_4$ 800 μL，持續攪拌。高溫組在室溫下攪拌一天後，加熱至 60℃ 持續 5 分鐘，即冷卻回室溫；低溫組立即放入 incubator 在 4℃環境下搖晃，並隔離光照。測樣品吸收與螢光光譜，以染料 DCM 為基準，計算 Q.Y.，比較合成時溫度對胰島素金奈米粒子螢光之影響。

2. 改變金離子濃度

取胰島素 10mg，溶於鹼性緩衝溶液 800 μL，持續攪拌，迅速加入 20 mg/mL HAuCl$_{4(aq)}$ 800 μL。立即將胰島素金奈米粒子溶液放入 incubator，在 4℃下搖晃，並隔離光照。重複上述步驟，但將 20 mg/mL HAuCl$_{4(aq)}$ 800 μL 換成加入前驅物【20 mg/mL HAuCl$_4$ $_{(aq)}$800 μL + 1 M NaOH $_{(aq)}$200 μL 】。以染料 DCM 為基準，測樣品之吸收與螢光光譜，計算 Q.Y.，比較合成時金離子濃度對胰島素金奈米粒子螢光之影響。

(三) 確認胰島素金奈米粒子

取胰島素 10 mg，溶於鹼性緩衝溶液中 800 μL，持續攪拌，迅速加入 20 mg/mL $HAuCl_{4(aq)}$ 800 μL。立即將胰島素金奈米粒子溶液放入 incubator，在 4℃ 下搖晃。

將所合成出來之胰島素金奈米粒子送測 Thermal Gravimetric Analysis (TGA)、粒徑分析儀、*Transmission electron microscopy* (TEM)、X-ray photoelectron spectroscopy (XPS)，以確認胰島素金奈米粒子大小與金奈米粒子價數。

因為胰島素是與細胞膜上的胰島素受體結合後，才得以進入細胞內，胰島素金奈米粒子的結構是否與胰島素相似便十分重要。因此測量胰島素與胰島素金奈米粒子的 far UV CD 光譜，觀察胰島素金奈米粒子二級結構是否與胰島素相似。

五、離子檢測

(一) 試驗各種離子對胰島素金奈米粒子的影響

為了測試胰島素金奈米粒子在生物體中對各種離子的反應，對胰島素金奈米粒子進行離子測試。

取之前製作的胰島素金奈米粒子，將其中的緩衝溶液置換成一般細胞培養所使用的 PBS。對多種陽離子進行定性測試，使用過氯酸鹽：K^+, Li^+, Ag^+, Mg^{2+}, Na^+, Cd^{2+}, Ca^{2+}, Hg^{2+}, Cu^{2+}, Ni^{2+}, Pb^{2+}, Fe^{3+}；對多種陰離子進行定性測試，使用鈉鹽：Br^-, F^-, I^-, NO_3^-, SCN^-, Cl^-, ClO_4^-, PO_4^{3-}, $P_2O_7^-$, acetate, benzoic acid, CN^-。

(二) 檢測溶液中氰離子

由之前實驗及 Elsner Equation 可知，胰島素金奈米粒子對氰離子反應特別明顯，應可偵測水溶液中氰離子，又反應系統皆在鹼性環境下，並不會

產生 HCN$_{(aq)}$。

Elsner Equation：$4Au + 8CN^- + O_2 + 2H_2O \rightarrow 4Au(CN)_2^- + 4OH^-$
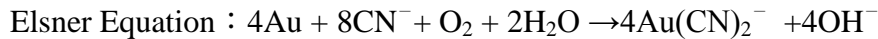
　　取之前製作的胰島素金奈米粒子，將其中的緩衝溶液置換成 PBS，並稀釋 15 倍。後取 1.5mL 測其吸收與螢光光譜。第一次先加入 10^{-3} M NaCN$_{(aq)}$ 2μL，混合均勻後，靜置五分鐘，測其吸收與螢光光譜。再逐步加入 10^{-3} M NaCN$_{(aq)}$，每次皆靜置五分鐘，再測其吸收與螢光光譜，直到紅色螢光光譜消失。

　　將數據繪製成圖表，以檢驗有無符合 Stern-Volmer 方程式，以做為對水中氰離子的檢測方法。

六、細胞測試

　　為了確認胰島素金奈米粒子具有生物活性，將細胞培養在胰島素金奈米粒子溶液中，以螢光檢測胰島素金奈米粒子是否進入細胞。因胰島素是經由與細胞膜上專一性受體結合後，進入細胞中促使細胞自血液中吸收葡萄糖。若胰島素金奈米粒子能與胰島素專一性受體結合，就能進入細胞內，也就表示胰島素金奈米粒子可代表胰島素在生物體內的狀況。

(一) 使用巨噬細胞 Raw264.7

　　因巨噬細胞會從環境胞吞許多物質，先使用巨噬細胞測試胰島素金奈米粒子是否可以進入細胞內。

　　將胰島素金奈米粒子餵入巨噬細胞，輔以染料 DAPI 標記細胞核、染料 FITC 標記細胞質位置。再把細胞玻片放入雙光子螢光顯微鏡下，以螢光觀察胰島素金奈米粒子是否進入細胞。

(二) 使用脂肪細胞 3T3-L1、肌肉細胞 C2C12

　　由文獻得知，脂肪細胞與肌肉細胞上有大量胰島素受體，因而選用脂肪細胞 3T3-L1 與已分化的肌肉細胞 C2C12，以取得胰島素金奈米粒子在細

胞中的螢光顯影圖像。

因為只有活的細胞可分解藍色的 MTT，使用 MTT (3-(4,5-Dimethylthiazol-2-Y1)-2,5-Diphemyltetrazolium Bromide) 做為細胞毒性測試的方法，測吸收度便可得知細胞存活率。將胰島素金奈米粒子對脂肪細胞 3T3-L1 進行 MTT 測試，確認毒性很低之後，將胰島素金奈米粒子餵入脂肪細胞、肌肉細胞，輔以染料 DAPI 標記細胞核位置、染料 FITC 標記細胞質位置。再把細胞玻片放入雙光子螢光顯微鏡下，以螢光觀察胰島素金奈米粒子是否進入細胞內。
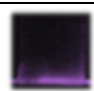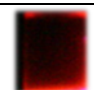
七、降血糖測試

為了更進一步確認胰島素金奈米粒子的生物活性，我們將市售之藥用 Humulin-regular 胰島素與自行合成之胰島素金奈米粒子，分別注射入各三隻白老鼠體內，實驗前後每隔三十分鐘抽血檢驗血糖濃度是否降低。

參、 研究結果與討論

一、 增進 BSA@Au 發螢光效率

(一) 使用還原劑

<center>表 3 BSA@Au 樣品編號</center>

編號	BSA(aq) (1mL)	HAuCl4(aq) (mg/mL)	(mL)	NaOH(aq) 1M(mL)	TBAB(aq) 0.1M(mL)	EtOH (mL)	攪拌時間	螢光顏色
A		----	----	----	----	----	5 min	
B		2	1	0.1	----	----	5 min	
C	50$_{mg/mL}$	20	1	1	----	----	4 hr	
D		20	1	1	1	----	5 min	
E		20	1	1	1	----	4 hr	
F	25$_{mg/mL}$	20	1	1	1	----	4 hr	
G	50$_{mg/mL}$	20	1	1	1	95%, 200	4 hr	

BSA 本身會發出波長 400nm 的藍色螢光(圖 1a)，但加入金離子後，螢光移至 465nm 處(圖 1b)，代表溶液中鮮有 BSA 蛋白質，而產生另一新物質，可能是 BSA 結構改變，抑或與金產生配位或鍵結。至於 B 與 D 的藍色螢光皆在同個區段，可推測是同一物質 B＝D。隨著反應時間拉長，E_1 藍色螢光比例下降，E_2 紅色螢光比例上升，可推測發出 λ_{max}=455nm 螢光的物質 E_1，可能為中間產物或不穩定結構(圖 1c)。添加還原劑會影響螢光波長，使有加還原劑的生成物 E，紅光波長較短。未加還原劑的 C，藍光部分波長與

<center>9</center>

BSA 一樣（圖 1d）。

圖 1 (a)BSA$_{(aq)}$螢光光譜，λ_{ex}=350nm，λ_{max}=400nm (b)BSA@Au(B、D)螢光光譜，λ_{ex}=350nm，λ_{max}=465nm (c)BSA@Au(E)螢光光譜， E$_1$：λ_{max}=455nm，E$_2$：λ_{max}=660nm (d) 比較 BSA@Au 因還原劑，而產生螢光之變化。(λ_{ex}=350nm)
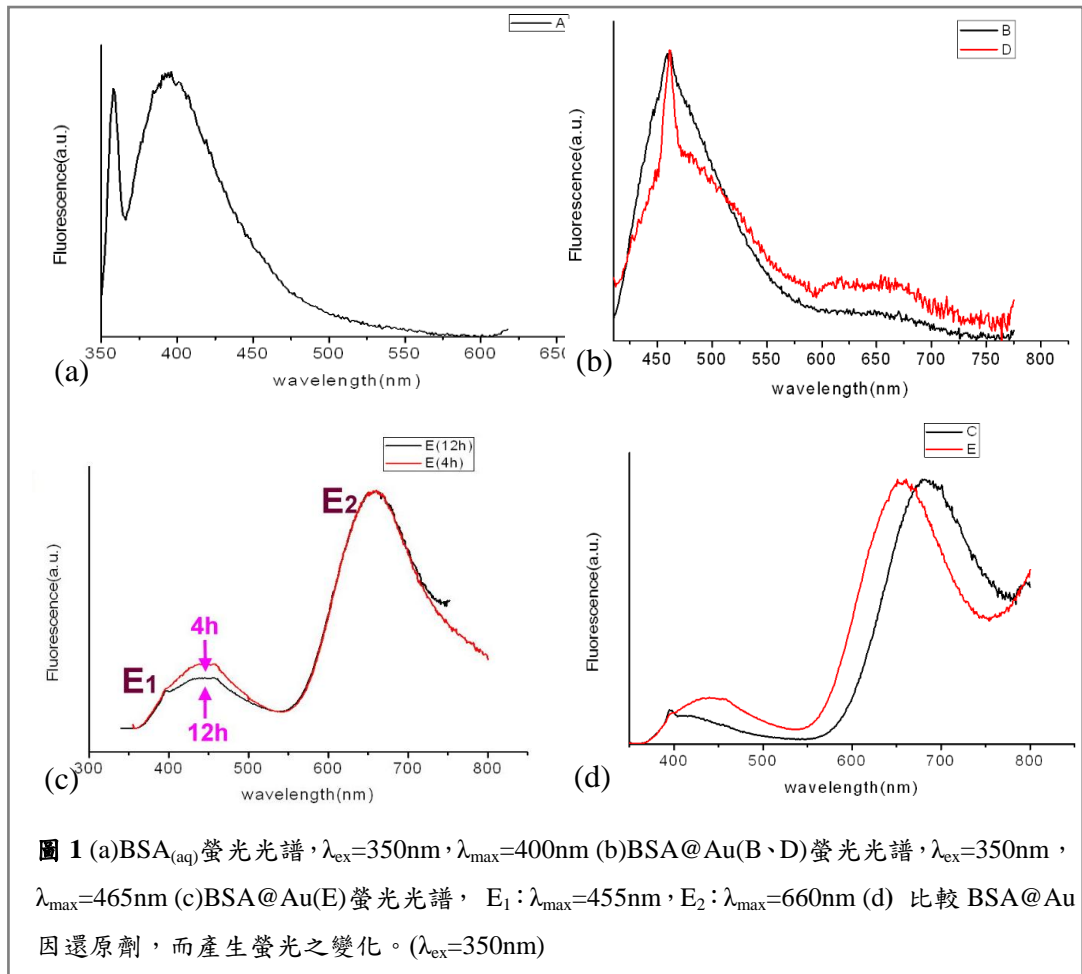
因此，推論還原劑 TBAB 會先使生成物 B＝D 轉變至中間產物 E1，再轉變至最後產物 E2，而不會讓生成物 B＝D 轉回反應物 BSA 放 400nm 的藍色螢光。將反應機制繪作圖 2，比較還原劑之影響：

Ⅰ： A＝C1→B＝D→C2 或者 A＝C1→B＝D→A＝C1；（沒加還原劑）

Ⅱ： A＝C1→B＝D→E1→E2。 （有加還原劑）
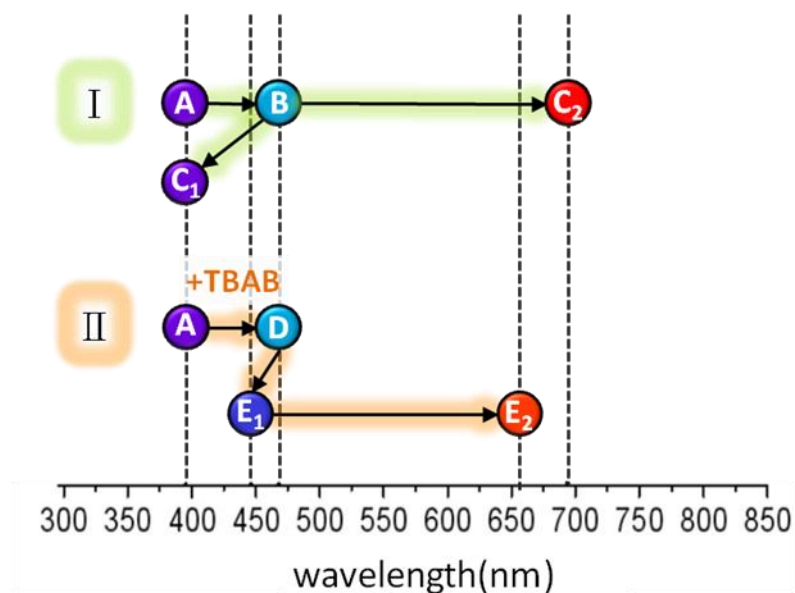
圖 2 BSA@Au 螢光反應過程示意圖

二、引入不同蛋白質

(一) 血清蛋白

表 4 不同血清蛋白之比較

蛋白質水溶液(1mL)		$NaOH_{(aq)}$(1mL)	$TBAB_{(aq)}$ (1mL)	$HAuCl_{4(aq)}$ (1mL)
HB	20mg/mL	0.5M	0.10M	20mg/mL
	20mg/mL	1.0M	0.10M	
	10mg/mL	1.0M	0.05M	
LGRM	100mg/mL	0.5M	0.10M	
	100mg/mL	1.0M	0.05M	
	20mg/mL	1.0M	0.10M	
	10mg/mL	1.0M	0.05M	
	10mg/mL	0.5M	0.05M	
MB	10mg/mL	1.0M	0.05M	
	20mg/mL	1.0M	0.10M	

所使用的血清蛋白所合成出的蛋白質金奈米粒子皆不會放出螢光,下一步嘗試使用易結晶之蛋白質,在結晶條件下使反應條件純化。

(二) 溶菌酶與胰島素

1. 製作溶菌酶金奈米粒子

已使用波長 300nm 的光激發溶菌酶，確認其無強烈螢光，不影響以波長 350nm 的光激發溶菌酶金奈米粒子所得到的光譜。調整合成溶菌酶之變因方式如下表。

表 5 調整合成溶菌酶金奈米粒子之變因

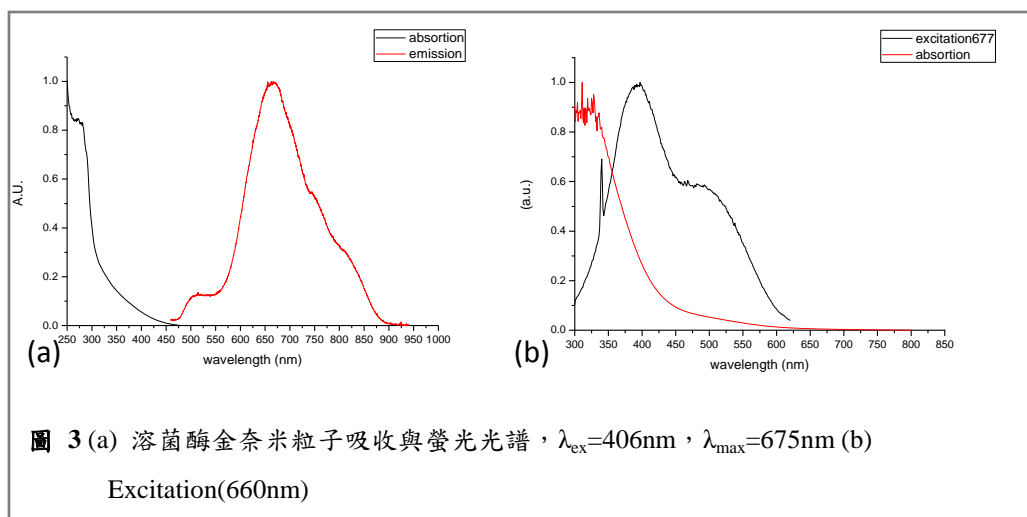| 溶菌酶$_{(aq)}$ (mL)		去離子水(mL)	NaOH$_{(aq)}$ 1M(mL)	TBAB$_{(aq)}$ 0.1M(mL)	NaCl$_{(aq)}$ 5% (mL)	HAuCl$_{4(aq)}$ 20$_{mg/mL}$(mL)
5 $_{mg/mL}$	1.000	0.500	0.250	----	----	0.250
10$_{mg/mL}$	0.500	0.500	0.500	----	----	0.500
	0.500	----	0.500	0.500	----	
	0.500	0.500	0.500	----	----	
	0.500	----	0.500	----	0.500	
	0.500	----	1.000	----	----	
	1.000	0.450	0.200	----	----	0.250
	5.000	5.000	5.000	----	----	5.000
	10.000	----	5.000	----	----	
18.4$_{mg/mL}$	1.000	0.900	0.050	----	----	0.050
		0.500	0.500	----	----	
50 $_{mg/mL}$	1.000	----	0.500	----	----	0.500

溶菌酶金奈米粒子螢光有兩個波峰，其 Q.Y.為 2% (圖 3a)。對 λ_{max}=677nm 做 excitation(圖 3b)，結果所得到的光譜與其吸收光譜不同。猜測激發光波段位於 400nm 前面，是由 λ_{max}=499nm 的螢光物質所吸收。

圖 3 (a) 溶菌酶金奈米粒子吸收與螢光光譜，λ_{ex}=406nm，λ_{max}=675nm (b) Excitation(660nm)

　　文獻資料顯示溶菌酶的結晶條件為 pH 值 4.5，但將會發光的溶菌酶奈米金置換至 50 mM Na(OAc) $_{(aq)}$, pH 值 4.5，出現混濁且不會發光。因酸性結晶條件與鹼性螢光條件相互抵觸，故暫不討論溶菌酶，另選擇胰島素。

2. 製作胰島素金奈米粒子

　　用波長 350nm 的光激發胰島素，只會在約 396nm 處有散射光，不影響波長 350nm 的光激發胰島素金奈米粒子所得到的光譜。調整合成胰島素金奈米粒子變因方式如下表 6。

表 6 調整合成胰島素金奈米粒子之變因-1

胰島素 (mg)	H_2O (mL)	Buffer(mL)	$NaOH_{(aq)}$ 1M(mL)	$HAuCl_{4(aq)}$ 20$_{mg/mL}$(mL)	$NaOH_{(aq)}$ 1×10^{-4}M(mL)	胰島素 濃度
7.3	1.85	----	0.100	0.05	----	3.63$_{mg/mL}$
7.3	1	NaCl150 Tris20 0.85	0.100	0.05	----	3.63$_{mg/mL}$
8.2	1.706	----	0.045	0.25	----	4.09$_{mg/mL}$
8.2	1.353	----	0.033	0.25	----	3.60$_{mg/mL}$
8.2	1	----	0.023	0.05	0.9275	4.09$_{mg/mL}$
8.2	5	----	0.500	0.25	4.6375	4.09$_{mg/mL}$
8.2	----	0.1 M	----	0.05	----	4.09$_{mg/mL}$

		Na$_2$HPO$_4$ /Na$_3$PO$_4$ 1.95			

　　從上表樣品挑選放紅光最強烈者（網底）做進一步實驗，但螢光依舊有兩個波峰，藍光部分有待再確認。配合結晶條件所用之緩衝溶液，全部改用 0.1M Na$_2$HPO$_{4(aq)}$/Na$_3$PO$_{4\ (aq)}$，避免多一個置換溶液的步驟之外，也為了維持胰島素金奈米粒子之穩定(表 7)。

表 7 調整合成胰島素金奈米粒子之變因-2　　　　　　　單位：mL

胰島素 8.2$_{mg/Ml(aq)}$	Buffer	1 M NaOH	20 $_{mg/mL}$ HAuCl$_4$	0.0001 M NaOH
1	----	0.0225	0.05	0.9275
1	----	0.0225	0.05	0.9275
1	0.9425	0.0075	0.05	----
1	0.9425	----	0.05	----
----	1.9425	----	0.05	0.9275
5	----	0.1125	0.25	4.6375
----	1.950	----	0.05	----

　　從有加緩衝溶液之樣本挑選，測量光譜隨時間之變化(圖 4)，發現在 0.5hr 時，也就是紅光即將要放螢光之際，吸收度在 250nm~300nm 間大增。推測需先有一吸收 250nm~300nm 波長的中間產物，再變成比較穩定的紅光胰島素金奈米粒子。
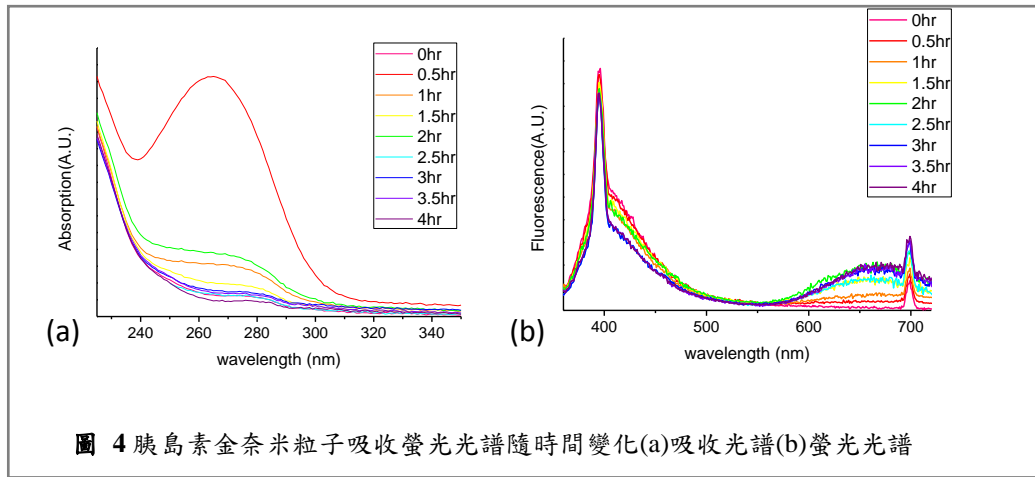
圖 4 胰島素金奈米粒子吸收螢光光譜隨時間變化(a)吸收光譜(b)螢光光譜

　　隨反應時間愈長，紅光增長，藍光消退。可能發藍光物質之物質，轉變成發紅光。在緩衝溶液中，胰島素金奈米粒子維持紅色螢光的時間較長，但紅光比例不如使用 NaOH$_{(aq)}$，是需再改善的部分。放螢光分四個階段：可將此結果當作參考，製作不同顏色的胰島素奈米金(圖 5、表 8)。
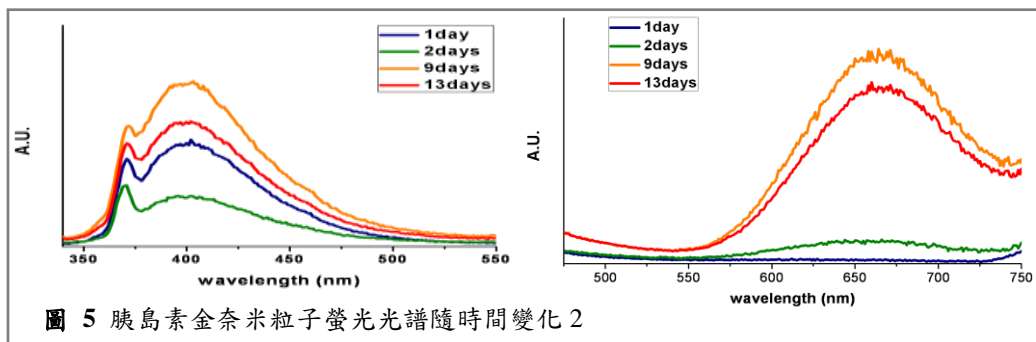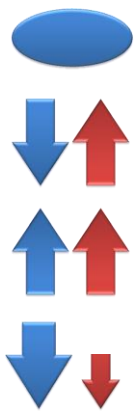

圖 5 胰島素金奈米粒子螢光光譜隨時間變化 2

表 8 胰島素金奈米粒子螢光顏色隨時間變化

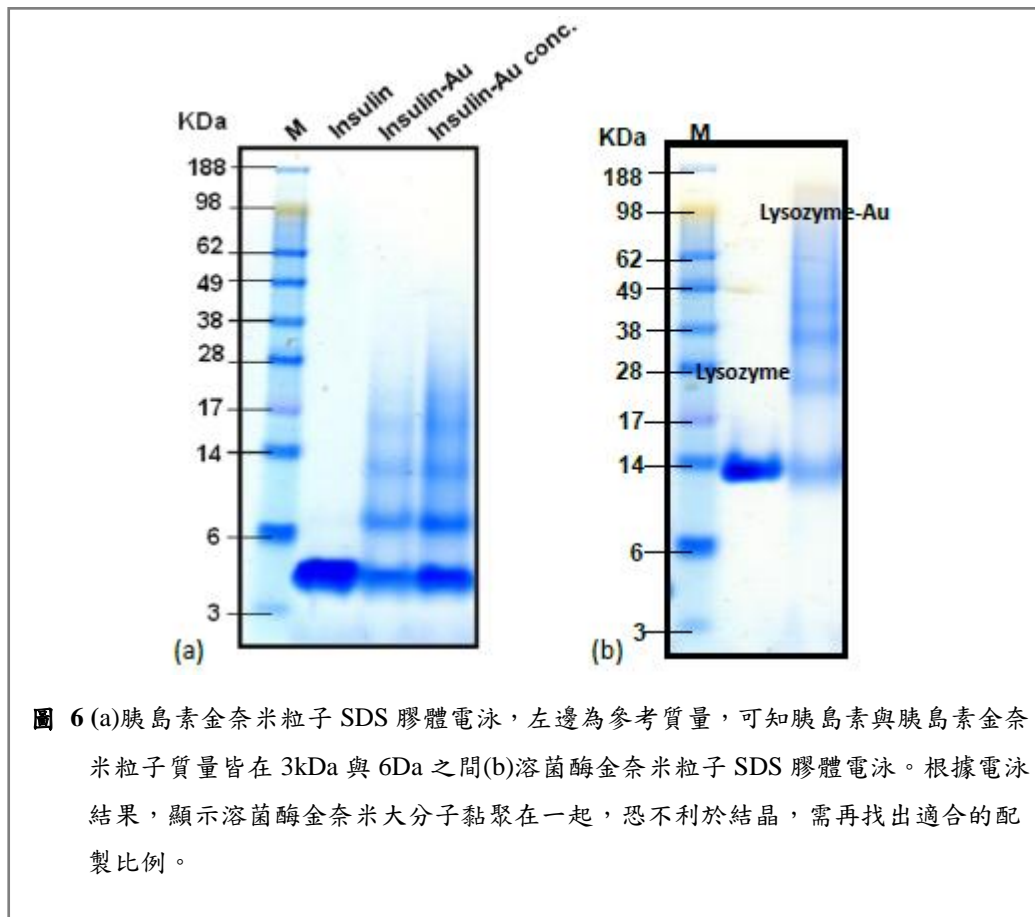| 光譜變化		呈現顏色	
⬭	只有藍光	藍色	
⬇⬆	藍光減弱，紅光出現	紫色	
⬆⬆	藍光、紅光一起增強	白色	
⬇⬇	藍光減弱、紅光減弱，惟藍光減弱速度較快。	粉紅色	

圖 6 (a)胰島素金奈米粒子 SDS 膠體電泳，左邊為參考質量，可知胰島素與胰島素金奈米粒子質量皆在 3kDa 與 6Da 之間(b)溶菌酶金奈米粒子 SDS 膠體電泳。根據電泳結果，顯示溶菌酶金奈米大分子黏聚在一起，恐不利於結晶，需再找出適合的配製比例。

　　胰島素金奈米粒子電泳結果較溶菌酶金奈米粒子較好，未膠黏成分子量數倍之分子(圖 6)，但 Q.Y.較差（1% ＜2% ）。

三、改善與測定胰島素金奈米粒子

(一) 胰島素金奈米粒子結晶

1. 製作胰島素結晶

表 9 Reservoirs

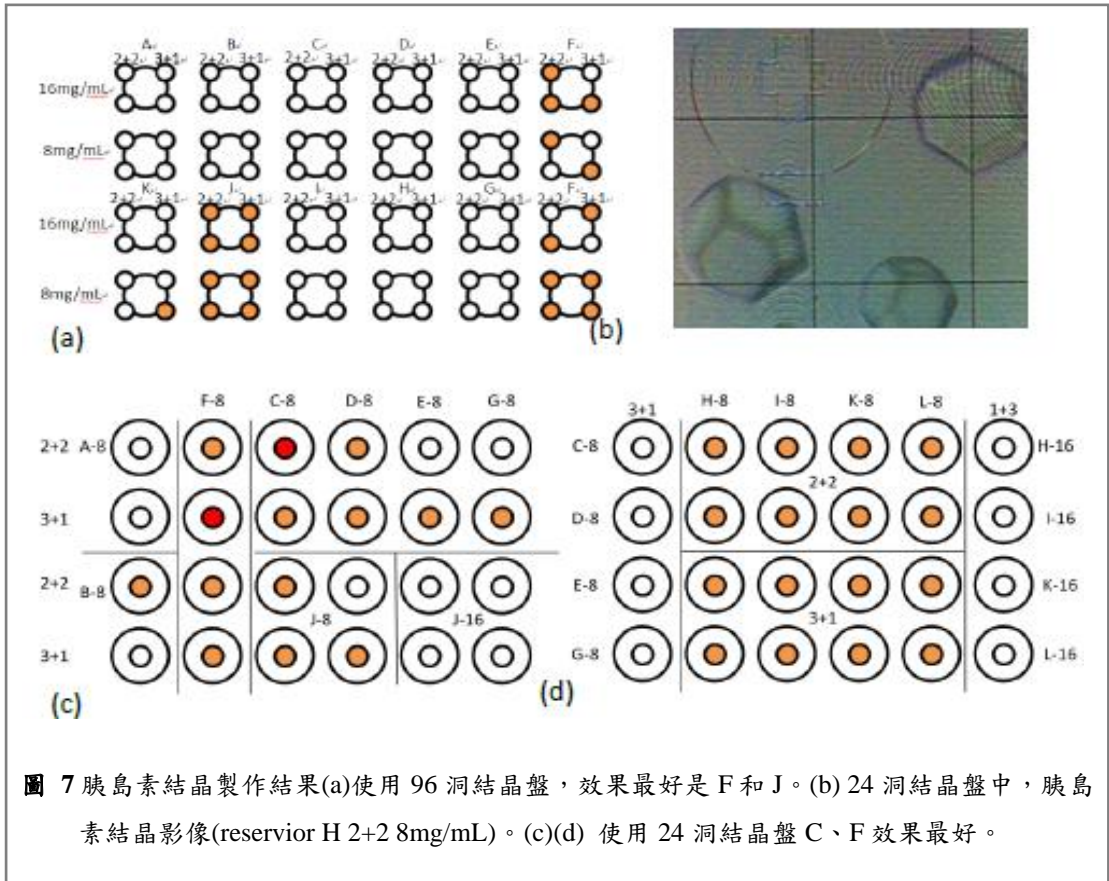| Reservoir 10mL	0.5 M $Na_2HPO_4(aq)$ (mL)	0.5 M $Na_3PO_4(aq)$ (mL)	去離子水 (mL)
A	5.250	1.750	3.000
B	5.625	1.875	2.500
C	6.000	2.000	2.000
D	6.375	2.125	1.500
E	6.750	2.250	1.000
F	9.344	0.000	0.656
G	7.125	2.375	0.500
H	7.500	2.500	0.000
I	7.500	2.500	0.000
J	9.000	0.000	1.000
K	6.390	2.130	1.480
L	0.000	9.344	0.656

圖 7 胰島素結晶製作結果(a)使用 96 洞結晶盤，效果最好是 F 和 J。(b) 24 洞結晶盤中，胰島素結晶影像(reservior H 2+2 8mg/mL)。(c)(d) 使用 24 洞結晶盤 C、F 效果最好。

製備不同濃度之 Reservoir：A～L(表 9)。

使用 96 洞結晶盤：如圖 7(a)(b)，橘色為有成功結晶之樣本，蛋白質濃度沒有太大差別，reserviors 中以 F、J 的效果最好。。

使用 24 洞結晶盤：如圖 7(c)(d)橘色為有成功結晶之樣本，紅色為晶形完整且大顆的樣本。用 8mg/mL、胰島素＋reservior（3μL+1μL）的濃度比較好。。

2. 胰島素金奈米粒子結晶

將胰島素結晶泡在 $HAuCl_{4(aq)}$ 溶液中，結構未損毀。(圖 8)
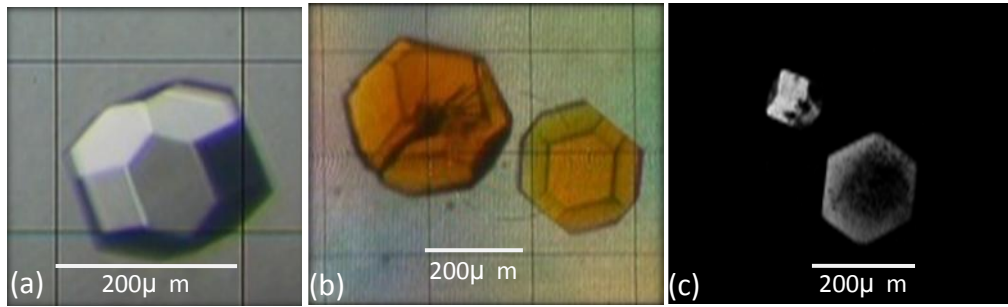
圖 8 胰島素-金結晶影像

3. 結晶光譜

　　相較溶液中無法偵測到胰島素之螢光，胰島素結晶後有藍色螢光(圖 9a)。胰島素-金結晶則是先放黃色螢光(圖 9b)，而後轉變成紅色螢光(圖 9c)。因胰島素金結晶放光與胰島素結晶不同，可知紅色螢光確實來自胰島素與金離子的交互作用，且結晶與水溶液中相同。晶體的螢光從黃色轉變至紅色，可見胰島素金奈米粒子螢光形成的階段性。
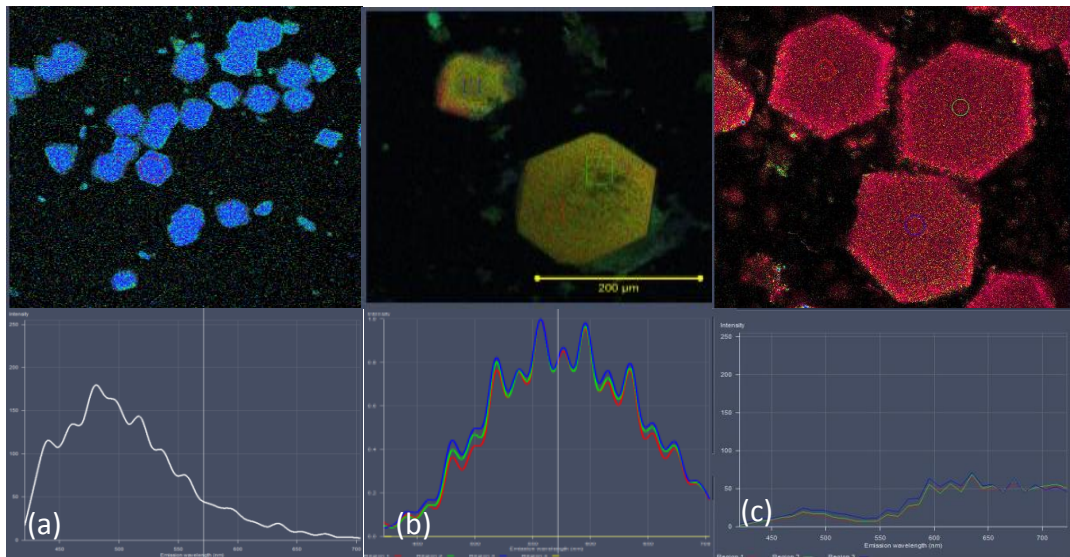
圖 9 (a)胰島素結晶螢光影像與光譜(λ_{ex}=405nm, λ_{max}=490nm)(b)第一階段胰島素金結晶螢光影像與光譜(λ_{ex}=405nm,λ_{max}=575nm) (c)第二階段胰島素金結晶螢光影像與光譜（λ_{ex}=406nm, λ_{max}=660nm)

(二) 提高胰島素金奈米粒子發光效率

1. 改變溫度

由圖 10 可知，在高溫下和在低溫下所合成的胰島素金奈米粒子，紅色的螢光較顯著，適合用在細胞測試上。相較於 37℃ 下所合成的螢光胰島素金奈米粒子 Q.Y. 為 1%，高溫和低溫組的有較高的 Q.Y. 2.04%。由於加熱胰島素易發生凝聚現象，恐無法進入細胞內，選用在 4℃ 製作的胰島素金奈米粒子進行後續實驗。

圖 10 (a)不同溫度下之胰島素金奈米粒子吸收與螢光光譜，（λ_{ex}=406nm）。(b)不同溫度下之胰島素金奈米粒子螢光影像。（λ_{ex}=365nm）
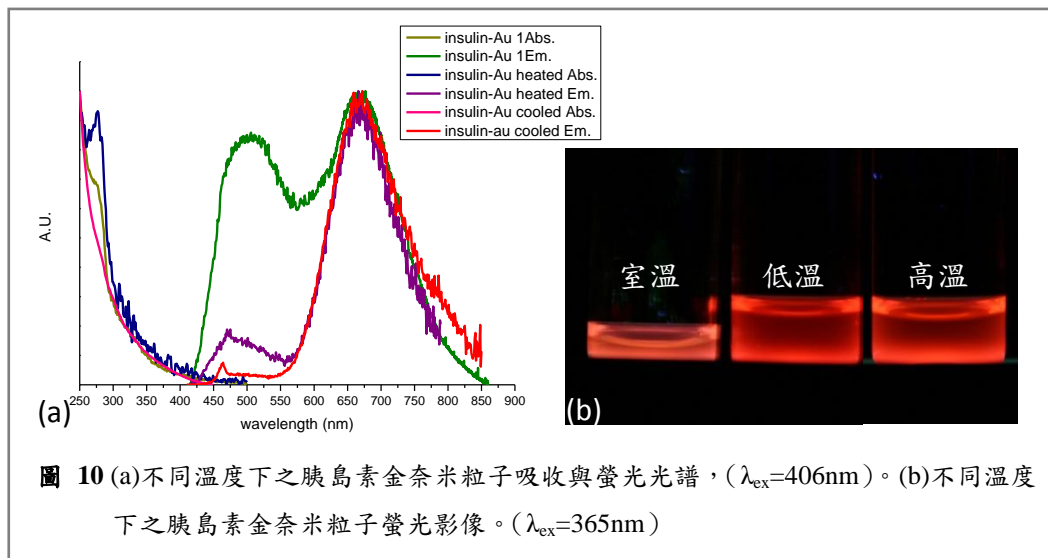
2. 改變金離子濃度

增加金離子濃度可使吸收度增高(圖 11a)，使紅色螢光明顯增加，Q.Y. 明顯由 2.04%上升至 3.55%(圖 11b)。
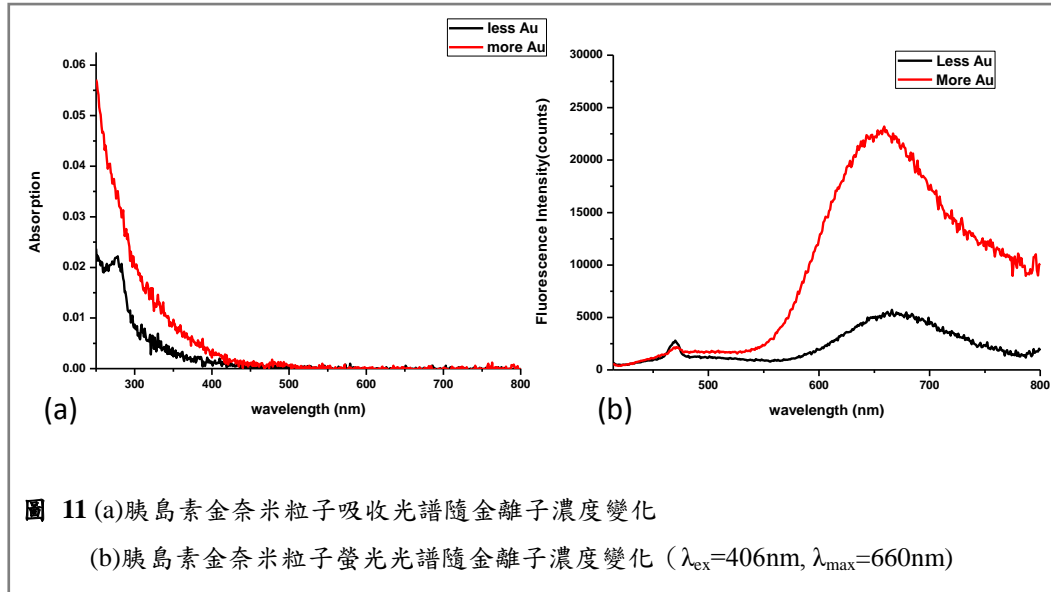
圖 11 (a)胰島素金奈米粒子吸收光譜隨金離子濃度變化

(b)胰島素金奈米粒子螢光光譜隨金離子濃度變化（λ_{ex}=406nm, λ_{max}=660nm）

(三) 確認胰島素金奈米粒子

　　經由 TEM，確認胰島素金奈米粒子中金奈米粒子大小約為 1nm(圖 12a)。

XPS 結果顯示: Au(0) 佔 75.7%，Au(I)佔 24.3%(圖 12b)。已知 Au 4f 7/2 的

結合能(binding energy)在 84.0 eV 和 85.1 eV 處會有特徵峰，分別代表 Au(0)

和 Au(I)。由此可以知道金奈米粒子表面有正一價金離子，幫助穩定金奈米

粒子。

(a)

(b)

12 (a)胰島素金奈米粒子 TEM 影像與元素分析。
(b)胰島素金奈米粒子之 binding energy。
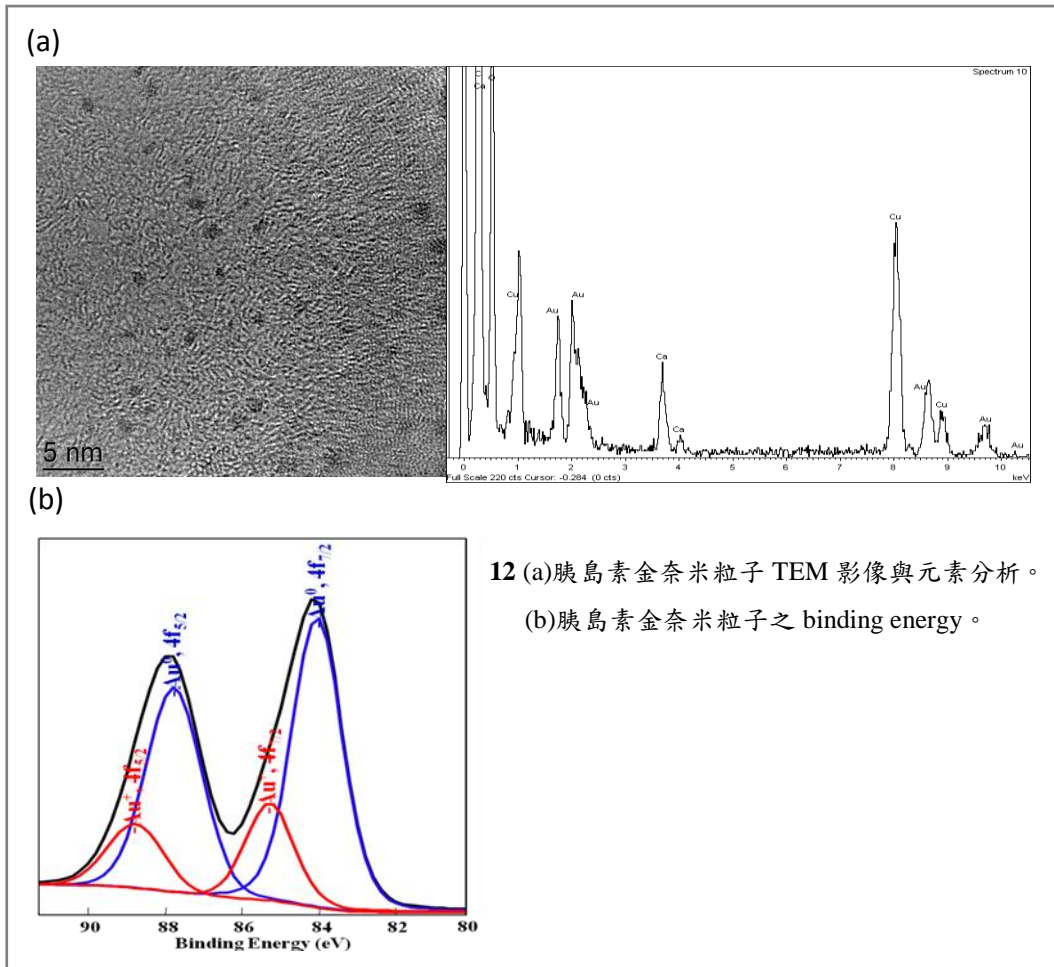
　　測量合成出來的胰島素與胰島素金奈米粒子的 CD(circular dichroism)

光譜結果，可知道胰島素金奈米粒子的二級結構相較於胰島素的二級結構

未變化太多，應可順利進行生物體應用。(圖 13d)

圖 13 (a)胰島素粒徑大小 3.0nm。(b)胰島素金奈米粒子粒徑大小為 5.7nm(c)為胰島素金奈米粒子送測 Thermal Gravimetric Analysis (TGA)的結果。(d)胰島素與胰島素金奈米粒子 CD 光譜比較。
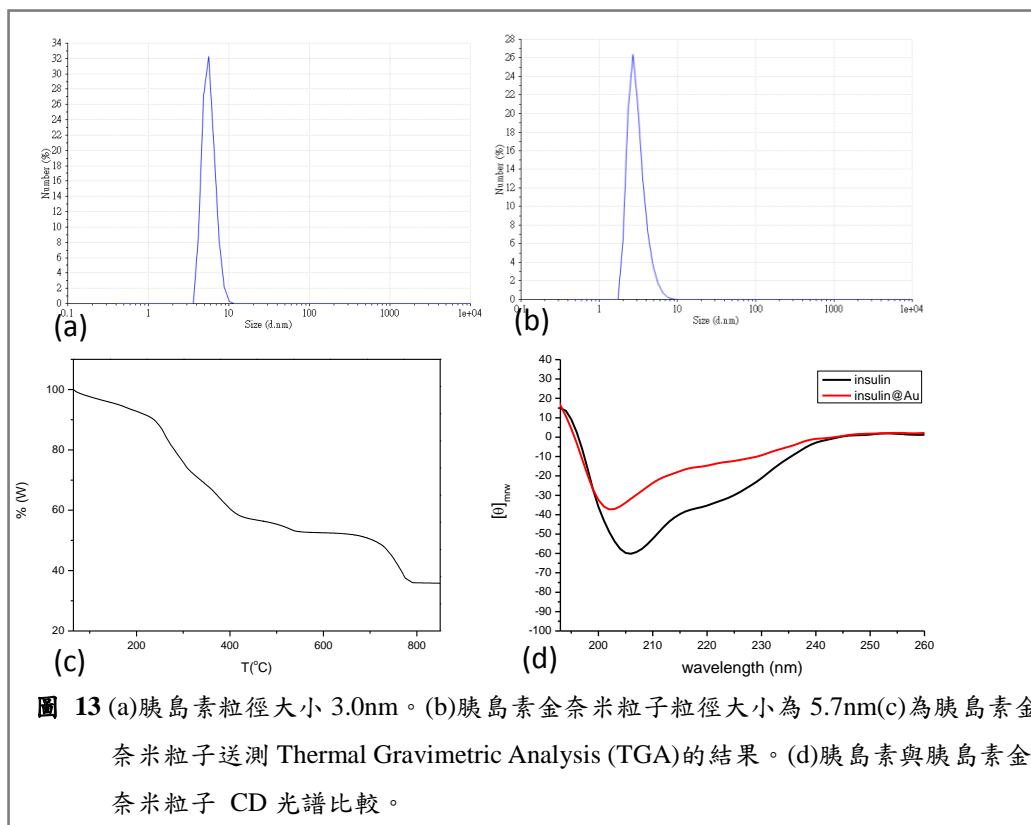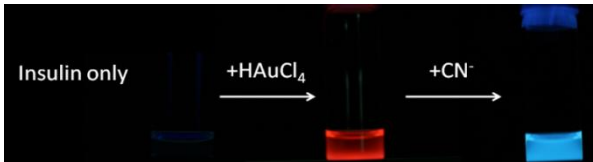
四、離子檢測

(一) 試驗各種離子對胰島素金奈米粒子的影響

下表為胰島素金奈米粒子對各種陽離子與陰離子的反應，可發現胰島素金奈米粒子遇到生物體中常見離子時非常穩定，但對氰離子有劇烈反應。

表 10 離子檢測

	螢光變化	離子種類
陽離子 (ClO_4^-)	紅色螢光變強	K^+, Li^+, Mg^{2+}, Na^+
	紅色螢光變弱	Cd^{2+}, Ca^{2+}
	紅色螢光變弱，產生沉澱	Hg^{2+}, Ag^+, Cu^{2+}, Ni^{2+}, Pb^{2+}, Fe^{3+}

23

| 陰離子
(Na⁺) | 紅色螢光變強 | Br⁻, F⁻, I⁻, NO₃⁻, SCN⁻, Cl⁻, ClO₄⁻, PO₄³⁻, P₂O₇⁻, acetate, benzoic acid |
| | 紅色螢光消失，
呈現藍色螢光 | CN⁻
  |

(二) 檢測溶液中氰離子

　　如圖 14，隨著加入越多的氰離子，由紅線到紫線，胰島素金奈米粒子的吸收度減弱，紅色螢光強度減弱，藍色螢光強度增強。

圖 14 (a)胰島素金奈米粒子吸收度隨氰離子濃度變化

　　(b)胰島素金奈米粒子螢光強度隨氰離子濃度變化，（λ_{ex}=406nm, λ_{max}=660nm）。
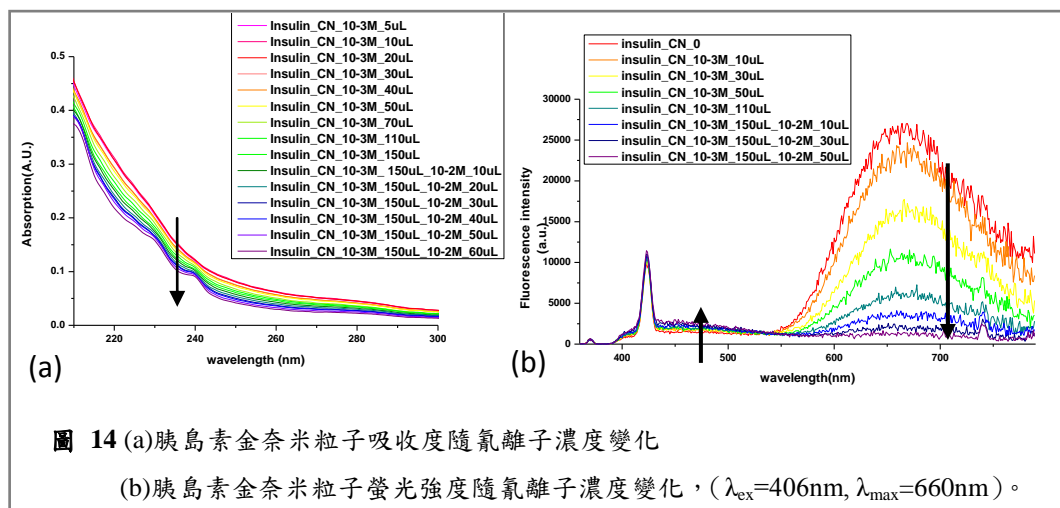
　　以氰離子在樣品中的濃度為 x 軸，以【原始紅色螢光強度 F_0/紅色螢光強度(F) 】為 y 軸，繪製成呈現線性關係的圖 15。目前測試到的最低濃度(2.49×10⁻⁶M)低於世界衛生組織所公布的水中氰離子濃度 2.7×10⁻⁶M，

但可用圖表推至更低的濃度，或使用未經稀釋的胰島素金奈米粒子。因此，可用胰島素金奈米粒子檢測水中氰離子濃度，特別是進入細胞內的生物檢測。
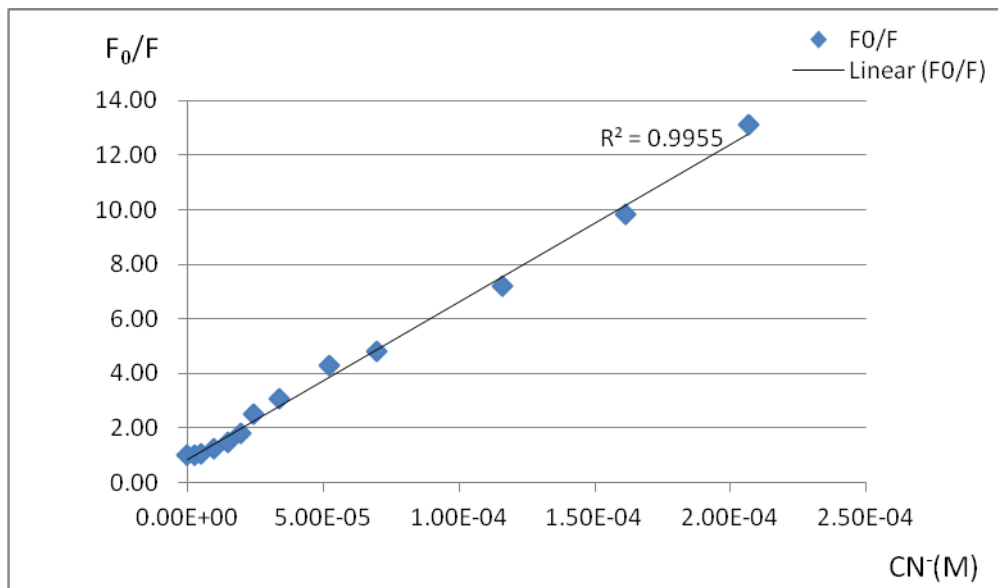
圖 15 Stern-Volmer plot of fluorescence quenching of the Au NCs by CN⁻

五、細胞測試

圖 **16** (a)胰島素金奈米粒子在巨噬細胞 Raw264.7 中放紅色螢光。(藍色螢光為細胞核)

(b)胰島素金奈米粒子對脂肪細胞 3T3-L1 之 MTT 細胞毒性測試結果。

(c)胰島素金奈米粒子溶液在細胞測試前之螢光影像。

(d)胰島素金奈米粒子在脂肪細胞 3T3-L1 中放紅色螢光。(藍色螢光為細胞核)

(e)胰島素金奈米粒子在分化肌肉細胞 C2C12 中放紅色螢光。(藍色螢光為細胞核,綠色螢光為細胞骨架)
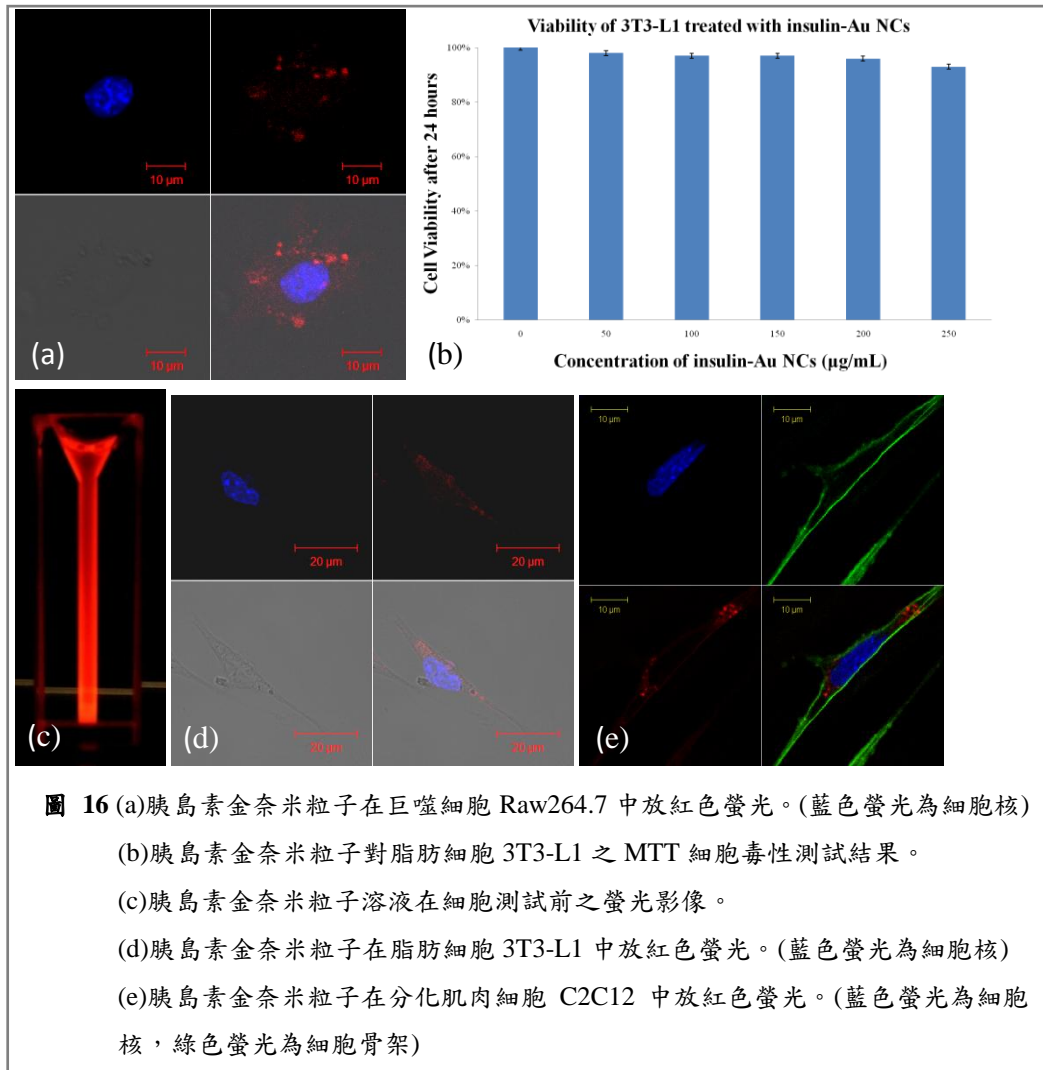
(一) 使用巨噬細胞 Raw264.7

如圖 16a,藍色為細胞核,綠色為細胞質,紅色為胰島素金奈米粒子。

圖片顯示胰島素金奈米粒子確實有進入細胞內。

(二) 使用脂肪細胞 3T3-L1、肌肉細胞 C2C12

如圖 16b,在 MTT 細胞測試中,胰島素金奈米粒子對於脂肪細胞 3T3-L1 的毒性是極低的。

圖 16(d)(e)顯示胰島素金奈米粒子可以確實進入細胞質中。因胰島素金奈米粒子進入細胞內的方法，只有經由細胞膜上的胰島素受體進入，代表胰島素金奈米粒子具有生物活性，日後可以藉由螢光觀察胰島素在細胞內的運作，比起傳統使用具有放射性的碘 [125] 安全許多。

六、降血糖測試

　　經由各三隻白老鼠的測試，將所合成的胰島素金奈米粒子與市售胰島素 Humulin-regular 比較，發現胰島素金奈米粒子確實可以如一般胰島素降低老鼠的血糖濃度。證明所合成之胰島素金奈米粒子在生物體內，確有生物活性，且可與胰島素發揮同等效益。
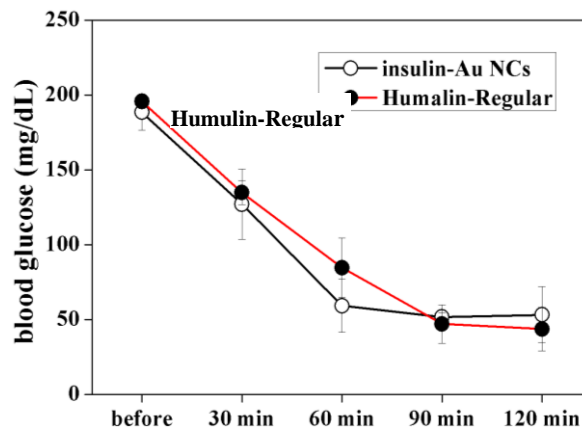
圖 17 胰島素金奈米粒子與市售胰島素降血糖效果比較。

肆、 結論與應用

一、BSA 金奈米粒子可發紅光（λ_{max}=約 660nm），其中添加還原劑可使生成物放光波長較短，影響反應機制及產物種類，使溶液中不會有從中間產物轉變的多餘牛血清白蛋白，提高產率。

二、由實驗得知胰島素金奈米粒子在溶液中會因 pH 值、緩衝溶液、金離子濃度、時間、溫度產生不同形式的放光。目前所合成出的最佳條件是取胰島素 10 mg，溶於鹼性緩衝溶液$_{(aq)}$ 800 μL，迅速加入 20 mg/mL HAuCl$_{4(aq)}$ 800 μL，立即放入 incubator 在 4℃環境下搖晃，並隔離光照。

三、透過胰島素金奈米粒子結晶，得到結晶狀態的胰島素金奈米粒子。

四、由 TEM、XPS 得知胰島素金奈米粒子中之金奈米粒子，直徑為 1nm，表面為一價金離子。由粒徑分析儀、CD 光譜，得知 5.7 nm 的胰島素金奈米粒子在生物體環境下，保持穩定，維持與胰島素相似結構。

五、經由檢量線結果，胰島素金奈米粒子可環保且低毒性地偵測水溶液、生物體中氰離子的濃度，偵測極限遠低於世界衛生組織所公告飲用水氰離子最低含量 $2.7×10^{-6}$ M，所以可做為 CN 檢測的應用試劑。

六、經由 MTT 細胞毒性測試，得知胰島素金奈米粒子對細胞毒性極低，且成功將胰島素金奈米粒子，經專一性受體餵入細胞內，證明胰島素金奈米粒子具有生物活性，且可使用細胞螢光顯影的技術，追蹤生物體內胰島素。相較傳統方法，可安全地用紅色螢光來觀察胰島素在細胞中狀況，以增進對胰島素作用機制的研究。

七、經由對老鼠之降血糖測試，證明所合成之螢光胰島素金奈米粒子，與胰島素降血糖之效果相同。所以可使用胰島素金奈米粒子在生物體內追蹤胰島素之

作用機制，以助於探討與胰島素相關疾病之機制。

伍、 未來展望

一、胰島素金奈米粒子應用在生物體內中之顯影追蹤。

二、可將胰島素金奈米粒子與磁性物質結合，合成具有光及磁性的雙功能性分
  子。

陸、 參考文獻

Benoit Dubertret, Michel Calame, and Albert J. Libchaber, **2001**, Single-mismatch
detection using gold-quenched fluorescent oligonucleotides, *Nature
Biotechnology, Vol. 19,* 365-370

Cheng-An J. Lin, Ting-Ya Yang, Chih-Hsien Lee, Sherry H. Huang, Ralph A.
Sperling, Marco Zanella, Jimmy K. Li, Ji-Lin Shen, Hsueh-Hsiao Wang, Hung-I
Yeh, Wolfgang J. Parak, and Walter H. Chang, **2009**, Synthesis, Characterization,
and Bioconjugation of Fluorescent Gold Nanoclusters toward Biological Labeling
Applications, *ACS Nano*, *3* (2), 395–401

Chih-Ching Huang, Cheng-Kang Chiang, Zong-Hong Lin, Kun-Hong Lee, and
Huan-Tsung Chang, **2008**, Bioconjugated Gold Nanodots and Nanoparticles for
Protein Assays Based on Photoluminescence Quenching, *Anal. Chem. 80*,
1497-1504

Chih-Ching Huang, Zusing Yang, Kun-Hong Lee, and Huan-Tsung Chang, **2007**,
Synthesis of Highly Fluorescent Gold Nanoparticles for Sensing Mercury(II),
Angew. Chem. , 119, 6948 –6952

Chi-Wei Liu, Chih-Ching Huang, and Huan-Tsung Chang, **2009**, Highly Selective DNA-Based Sensor for Lead(II) and Mercury(II) Ions, *Anal. Chem.*, *81,* 2383–2387

Hui Wei, Zidong Wang, Limin Yang, Shiliang Tian, Changjun Hou and Yi Lu, **2010**, Lysozyme-stabilized gold fluorescent cluster: Synthesis and application as Hg^{2+} sensor, *Analyst, 135*, 1406–1410

J. w. S. Morris, Daniel A. Mercola and Edward Arquilla, **1968**, An Analysis of The Near Ultraviolet Circular Dichroism of Insulin, *Biochem. Biophys. Acta, 160*, 145-150

Jianping Xie, Yuangang Zheng and Jackie Y. Ying, **2008**, Highly selective and ultrasensitive detection of Hg^{2+} based on fluorescence quenching of Au nanoclusters by Hg^{2+}–Au^+ interactions, *Chem. Commun., 46*, 961–963

Jianping Xie, Yuangang Zheng, and Jackie Y. Ying, **2009**, Protein-Directed Synthesis of Highly Fluorescent Gold Nanoclusters, *J. Am. Chem. Soc.*, *131 (3)*, 888-889

Kadir Aslan, Joseph R. Lakowicz, and Chris D. Geddes, **2004**, Nanogold-plasmon-resonance-based glucose sensing, *Analytical Biochemistry, 330*, 145–155

Li Shang, Lihua Jin and Shaojun Dong, **2009**, Sensitive turn-on fluorescent detection of cyanide based on the dissolution of fluorophore functionalized gold nanoparticles, *Chem. Commun., 2009*, 3077–3079

Mario Bouchard, Jesus Zurdo, Ewan J. Nettleton, Christopher M. Dobson, and Carol V. Robinson, **2000,** Formation of insulin amyloid fibrils followed by FTIR

simultaneously with CD and electron microscopy, *Protein Science*, *9*, 1960–1967

Mei-Lin Ho, Jia-Ming Hsieh, Chih-Wei Lai, Hsin-Chieh Peng, Chia-Cheng Kang, I-Che Wu, Chin-Hung Lai, Yu-Chun Chen, and Pi-Tai Chou, **2009**, 15-Crown-5 Functionalized Au Nanoparticles Synthesized via Single Molecule Exchange on Silica Nanoparticles: Its Application to Probe 15-Crown-5/K+/15-Crown-5 "Sandwiches" as Linking Mechanisms, *J. Phys. Chem. C*, *113,* 1686–1693

Nina V. Visser, Mark A. Hink, Jan Willem Borst, Gerard N.M. van der Krogt, Antonie J.W.G. Visser, **2002**, Circular dichroism spectroscopy of fluorescent proteins, *FEBS Letters, 521*, 31-35

Olga Gursky, Youli Li, John Badger, and Donald L. D. Caspar, **1992**, Monovalent cation binding to cubic insulin crystals, *Biophys. J. Biophysical Society, Vol. 61* 604-611

Ralf Jansen, Wojciech Dzwolak, and Roland Winter, **2005**, Amyloidogenic Self-Assembly of Insulin Aggregates Probed by High Resolution Atomic Force Microscopy, *Biophysical Journal, 88,* 1344–1353

Sarah H. Radwan and Hassan ME Azzazy, **2009**, Gold Nanoparticles for Molecular Diagnostic, *Expert Rev. Mol. Diagn. 9(5)*, 511-524

Sharon M. Kelly, Thomas J. Jess, Nicholas C. Price, **2005**, How to study proteins by circular dichroism, *Biochimica et Biophysica Acta 1751* , 119 – 139

Sheng Yao, Hyo-Yang Ahn, Xuhua Wang, Jie Fu, Eric W. Van Stryland, David J. Hagan, and Kevin D. Belfield, 2010, Donor-Acceptor-Donor Fluorene Derivatives for Two-Photon Fluorescence Lysosomal Imaging, *J. Org. Chem. , 75*, 3965–3974

Shuji Sato, Charles D. Ebert, and Sung Wan Kim, **1983**, Prevention of Insulin

Self- Association and Surface Adsorption, *Journal of Pharmaceutical Sciences*, *Vol. 72,* No. 3

Stephen P. Wood and Thomas L. Blundell, **1975**, The Relation of Conformation and Association of Insulin to Receptor Binding;X-Ray and Circular-Dichroism Studies on Bovine and Hystricomorph Insulins, *Eur. J. Biochem. ,55,* 531-542

Tao Liu, Ji'an Tang, and Long Jiang, **2004**, The enhancement effect of gold nanoparticles as a surface modifier on DNA sensor sensitivity, *Biochemical and Biophysical Research Communications, 313*, 3–7

Uwe H. F. Bunz and Vincent M. Rotello, **2009**, Gold Nanoparticle–Fluorophore Complexes: Sensitive and Discerning "Noses" for Biosystems Sensing, *Angew. Chem., 49*, 3268 – 3279

Victoria Sluzky, Janet A. Tamada, Alexander M. Klibanovt, and Robert Langer, **1991**, Kinetics of insulin aggregation in aqueous solutions upon agitation in the presence of hydrophobic surfaces, *Proc. Nati. Acad. Sci. USA Vol. 88*, 9377-9381

Vincent Du Vigneaud, **1927**, The Sulfur Of Insulin, *J. Bio. Chem., LXXV No.2*

Yanlan Liu, Kelong Ai, Xiaoli Cheng, Lihua Huo, and Lehui Lu, **2010**, Gold-Nanocluster-Based Fluorescent Sensors for Highly Sensitive and Selective Detection of Cyanide in Water, *Adv. Funct. Mater. , 20*, 951–956

Yee-Hsiung ChenJ Jen Tsi Yang, and Hugo M. Martinez, **1972**, Determination of the Secondary Structures of Proteins by Circular Dichroism and Optical Rotatory Dispersion, *Biochemistry, Vol . 11, No. 22*

評語

1. 題目有相當的創意，生物方向的應用具有一定程度的潛力。

2. 產物的鑑定宜更加完整。

3. 生物應用的數據宜更加完整。

Lighting Insulin with Gold Nanodots

CH010

Yun-Chen Chien

Taipei First Girls High School, Taipei, CHINESE TAIPEI

Abstract

As more people suffer from diabetes, understanding the key mechanism and improving the treatments are crucial.   Regarding this problem, a convenient and efficient method is designed to trace the key protein insulin in diabetes *in vivo*, by synthesizing the fluorescent insulin-Au nanodots.

In order to achieve the sufficient fluorescence efficiency of insulin-Au nanodots without denaturation, optimization with red fluorescence (λmax=660nm) is conducted.

The advantages of insulin-Au nanodots are proved to be the following.   Compared to organic dyes, gold nanodots allow real-time tracing and much less photobleaching.   The synthesized insulin-Au nanodots are capable of binding with insulin receptor and getting into cells as insulin does, demonstrated by the fluorescent insulin-Au nanodots and glucose uptakes.   With comparable biological activity to that of insulin and low cytotoxicity, the fluorescent insulin-Au nanodots are competent markers *in vitro* or even *in vivo*.

§ Introduction

Insulin relates to many diseases, including diabetes, Alzheimer's disease, obesity and aging. Its signaling pathway controls the growth of an organism, and hence exerts a profound influence on metabolism and reproduction.[1] However, current method cannot provide the instant distribution of the key protein insulin without invasive study or isotope use. Regarding this problem, a convenient and efficient method is designed to trace insulin by synthesizing the fluorescent insulin-Au nanodots.

Fluorescent properties of gold clusters are observed at sizes under 2 nm.[2] Compared to organic dyes, gold nanodots allow real-time tracing and much less photobleaching.[3] Recently, synthesizing fluorescent gold nanonanodots with biological molecules coating has been developed.[4][5] It inspired me to use insulin as both template and stabilizer to synthesize fluorescent insulin-gold nanodots (insulin-Au nanodots). By tracing the fluorescent insulin-Au nanodots, we can learn more about the role insulin plays in those diseases.

§ Experimental Procedures

1. Synthesis of the fluorescent insulin-Au nanodots

(A) Synthesis

Bovine pancreas insulin was purchased from Sigma. The insulin-Au nanodots were synthesized through reduction of Au with insulin, as a soft template, from hydrogen tetrachloroaurate (III) trihydrate ($HAuCl_4 \cdot 3H_2O$) in aqueous 0.1 M $Na_3PO_{4(aq)}$ buffer at pH 10.4. By reacting with insulin for 12 hours in the dark at 4℃, red-emissive insulin-Au nanodots were generated. The optimized procedure above was found after temperature, pH value, reaction time and concentrations were adjusted to achieve the sufficient quantum yield (Q.Y.) and maintain the bioactivity of insulin. The crude products were then purified by centrifugal filtration (4000×g) for 30 min with a cutoff of 5 kDa to obtain the insulin-Au nanodots for subsequent applications.

Steady-state absorption and emission spectra of insulin-Au nanodots were recorded with spectrophotometer (U-3310, Hitachi) and fluorimeter (FS920, Edinburgh), respectively. The spectral responses of excitation and emission of the fluorimeter were both calibrated. The emission Q.Y. of insulin-Au nanodots is determined by comparison method in which [4-(Dicyanomethylene)-2-methyl-6- (4-dimethylaminostyryl)-4H-pyran] (DCM dye) solution in methanol with known Q.Y. of ~0.44 served as a standard. Emission lifetime measurement was performed with fluorimeter comprising a built-in time-correlated single photon-counting system and a pulsed hydrogen or nitrogen lamp as the excitation source. Kinetic data were analyzed by using an iterative least-squares fitting procedure in combination with a deconvolution method, allowing partial removal of the instrumental time-broadening and providing a temporal resolution of approximately 300 ps. The emission decay was fitted with sum of exponential functions.

(B) Characterization

The insulin crystals were grown using the sitting drop vapor diffusion method at 25 ℃. A drop contained 15 mg/mL insulin dissolved in 0.1 M Na_2HPO_4/Na_3PO_4 at pH 10.4. The reservoir solution was 0.425 M Na_2HPO_4/Na_3PO_4. 1 mM $HAuCl_4$ (pH 10.4) was added into an aqueous solution containing insulin crystal to make insulin-Au crystals. The images and spectra of crystals were recorded by confocal fluorescence microscopy (LSM710 NLO, Zeiss).

The size of insulin-Au nanodots was determined by transmission electron microscope (TEM, JEM 1230, JEOL) operated at 200 kV and dynamic light scattering (DLS) in order to determine their shape, dimension and size distribution. The specimen is prepared by drop-casting the Au nanodots suspension on a Cu-grid-supported quantifoil. By observing the casted materials at the hole area of the supporting film, background-less image is then obtained.

X-ray photoelectron spectrometry (XPS) was used to determine the chemical state of Au. Au nanodots were drop-casted on a Si wafer. The spectra were recorded with a scanning ESCA microprobe (PHI 5000 VersaProbe, ULVAC-PHI) using a micro-focused, monochromatic Al Kα X-ray (25 W, 100 μm). The take-off angle of the photoelectron was 45°. A dual beam charge neutralizer (Ar^+ gun and flooding electron beam) was used to compensate the charge up effect.

2. Biological activity of insulin-Au nanodots

(A) Cytotoxicity

The cellular toxicity of insulin-Au nanodots was evaluated by using a colorimetric assay agent, 3-(4,5-dimethylthiazol-2-yl)-2,5-diphenyltetrazolium bromide (MTT, Roche). Mouse C2C12 myoblast cells were seeded on a 10 cm petri dish with 3×10^6 cells per well in Dulbecco's modified Eagle's medium (DMEM, Gibco) supplemented with 10% heat-inactivated fetal bovine serum (FBS, Gibco). For cell expansion, the cells were cultured under the atmosphere of 5% CO_2 at 37.0℃. Cells were passed through trypsinization, and nucleated cells were centrifuged at 1000×g for harvesting. For cytotoxicity test, cells were seeded in a 24-well plate with density of 3×10^4 cells/well in 1 mL DMEM to promote the uptake of the particles. For contrast with control group, five different concentrations (250, 200, 150, 100, and 50 μg/mL) of insulin-Au nanodots were added to the cells. After 24 hours of incubation at 37.0℃, each well was washed with phosphate-buffered saline (PBS, 137 mM NaCl, 2.68 mM KCl, 10 mM Na_2HPO_4, 1.76 mM KH_2PO_4, pH 7.4) twice, and incubated with 500 μL DMEM with 10% of MTT agent for 3 hours. After removal of the medium, the newly formed purple MTT-formazan was dissolved in 300 μL dimethyl sulfoxide (Sigma-Aldrich) and the absorbance was measured at 595 nm with a microplate reader (BIO-RAD model 680, VERSA Max). A total of three replicates were performed.

(B) Binding with receptors

The cellular bindings and uptake of insulin-Au nanodots was determined by laser-scanning confocal fluorescence microscopy (LSM710 NLO, Zeiss). For confocal microscopic study, C2C12 myoblast cells were seeded in a 6 well plate at 3×10^4 cells/well density in 2 mL DMEM. After 30 min incubation with 250 μg/mL of Au nanodots, cells were washed three times with PBS and then fixed by 3.7% paraformaldehyde in PBS at room temperature for 10 min. The cells were then washed twice with PBS and incubated with 0.1% Triton X-100 (Sigma-Aldrich) plus 3% BSA (Sigma-Aldrich) in PBS at room temperature for 5 min. 4',6-diamidino-2-phenylindole (DAPI, Molecular Probes) and Alexa Fluor® 488 phalloidin were used in this optical microscopic study for nucleus and actin labeling, respectively. Before 10 μg/mL DAPI staining in PBS for 5 min at room temperature, cell samples were washed with PBS twice and then examined with confocal spectral microscopeequipped with 63X (P-APO, 1.40 Oil immersion) objective, and using 405 nm Diode laser, 488 nm Argon laser, and 543 nm He-Ne laser as excitation source.

(C) Glucose uptakes of cells

L6 rat skeletal muscle cells were cultured in DMEM with 2% FBS to differentiate. Cells were plated at 1×10^5/well in 12-well plates and maintained at 37.0℃ in a humidified 5% CO_2 environment. The glucose uptake of fluorescemt glucose analog, [2-(N-(7-nitrobenz -2-0xa-1,3-diazol-4-yl)amino)-2-deoxyglucose] (2-NBDG) was determined with a multilabel counter (Victor 1420, Wallac). The cells were incubated with 300 μM 2-NBDG together with 100 nM insulin or 100 nM insulin-Au, respectively for 30 min at 37.0℃. Cells cultured in 12-well plate were washed with Krebs-Ringer bicarbonate buffer (KRP buffer) and then dissolved in 0.1% SDS at room temperature for 5 min. 200 μL solution from each well was added into black plate for absorption measurement at 485nm and 535 nm. The protein content was measured by trypan blue (Sigma), using bovine serum albumin (BSA, Sigma) as a standard protein.

§ **Results and Discussion**

1. Synthesis of the fluorescent insulin-Au nanodots
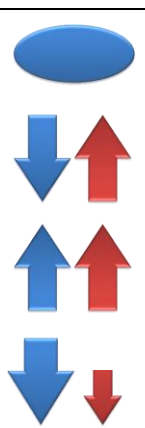
(A) Synthesis

As the reaction time at room temperature increased, the luminescence color of insulin-Au nanodots changed gradually from blue to red under 365 nm UV light. This implies that there is a blue fluorescent intermediate before insulin-Au nanodots reach the stability with red fluorescence [Table 1, Fig. 1 (a), (b)]. For future applications of insulin tracing *in vivo*, the wavelength of the emission should be long enough to get through the tissue without too much absorption.
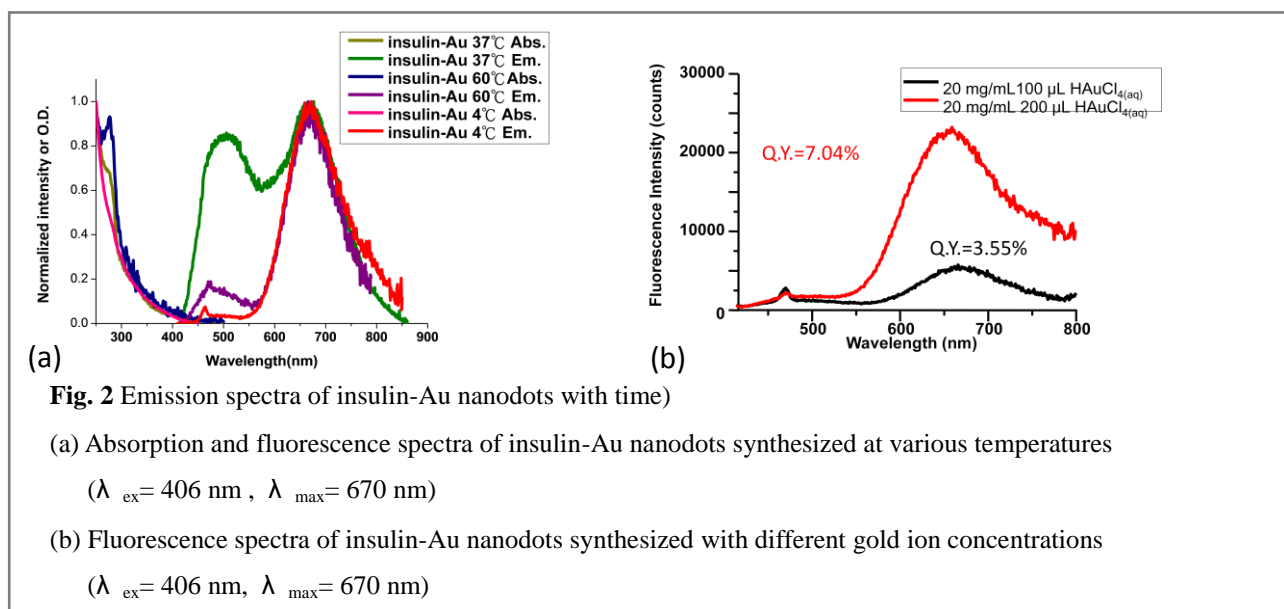
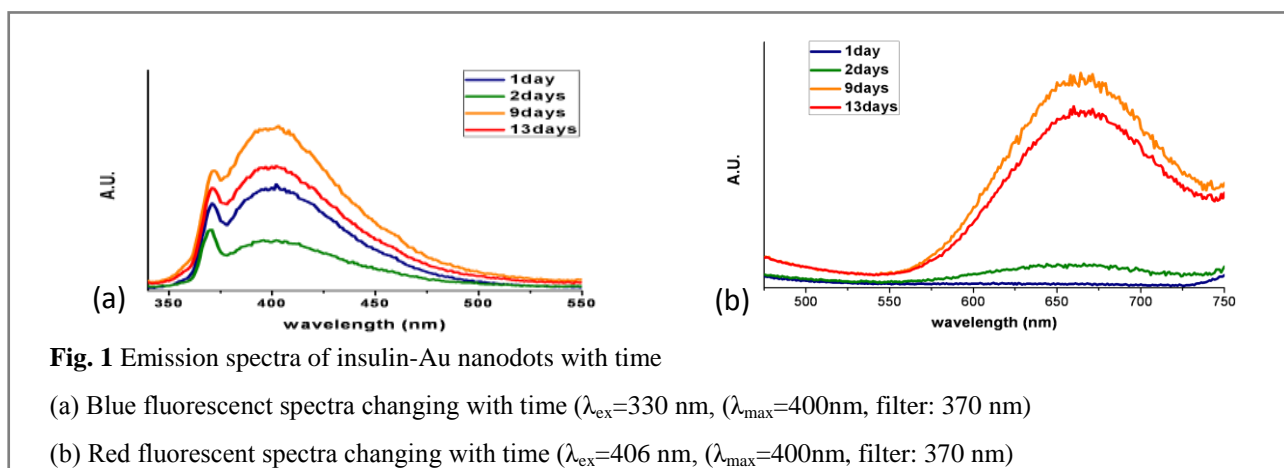The temperature affected the Q.Y. and red light percentage. Although insulin-Au nanodots synthesized at both 4℃ and 60℃ showed better Q.Y. than those synthesized at room temperature, the best synthesis temperature is at 4℃ because the strucuture of insulin remains native under low temperature [Fig. 2 (a)].

When using 5 mg/mL insulin, the Q.Y of insulin-Au nanodots synthesized with 200 μL HAuCl$_{4(aq)}$ (20 mg/mL) is better than those synthesized with 100 μL HAuCl$_{4(aq)}$ (20 mg/mL) [Fig. 2 (b)].

The optimized procedure is to add insulin 10 mg in buffer (pH 10.4, 800 μL) and HAuCl$_{4(aq)}$ (20 mg/mL, 200 μL) at 4℃ for 12 hr.

Table 1　Luminescent color of insulin-Au nanodots

			Color	
		Only blue fluorescence exists	blue	
		Blue fluorescence decays; red fluorescence shows up.	purple	
		Both blue and red fluorescence increase.	white	
		Both blue and red fluorescence decay.	pink	

Fig. 1 Emission spectra of insulin-Au nanodots with time

(a) Blue fluorescenct spectra changing with time (λ_{ex}=330 nm, (λ_{max}=400nm, filter: 370 nm)

(b) Red fluorescent spectra changing with time (λ_{ex}=406 nm, (λ_{max}=400nm, filter: 370 nm)

Fig. 2 Emission spectra of insulin-Au nanodots with time)

(a) Absorption and fluorescence spectra of insulin-Au nanodots synthesized at various temperatures

(λ_{ex} = 406 nm , λ_{max}= 670 nm)

(b) Fluorescence spectra of insulin-Au nanodots synthesized with different gold ion concentrations

(λ_{ex} = 406 nm, λ_{max}= 670 nm)

(B) Characterization

The completed insulin crystals were grown [Fig. 3 (a)] and then added into the solution containing 1 mM $HAuCl_{4(aq)}$ without destruction [Fig. (b), (c)]. The fluorescence of insulin crystals is blue (λ_{max}=490nm), which can explain the blue fluorescence measured in solution was from aggregate insulin. The fluorescence of insulin-Au nanodots gradually changed from yellow (λ_{max}=575nm) [Fig. 2 (e), (h)] to red and finally reach similar peak (λ_{max}=670nm) to the fluorescence of insulin-Au nanodots in solution (λ_{max}=670nm) [Fig. 2 (f), (i)]. The highly ordered protein assembly with nano-sized solvent-filled pores makes insulin crystals capable of promoting Au nanodots formation.
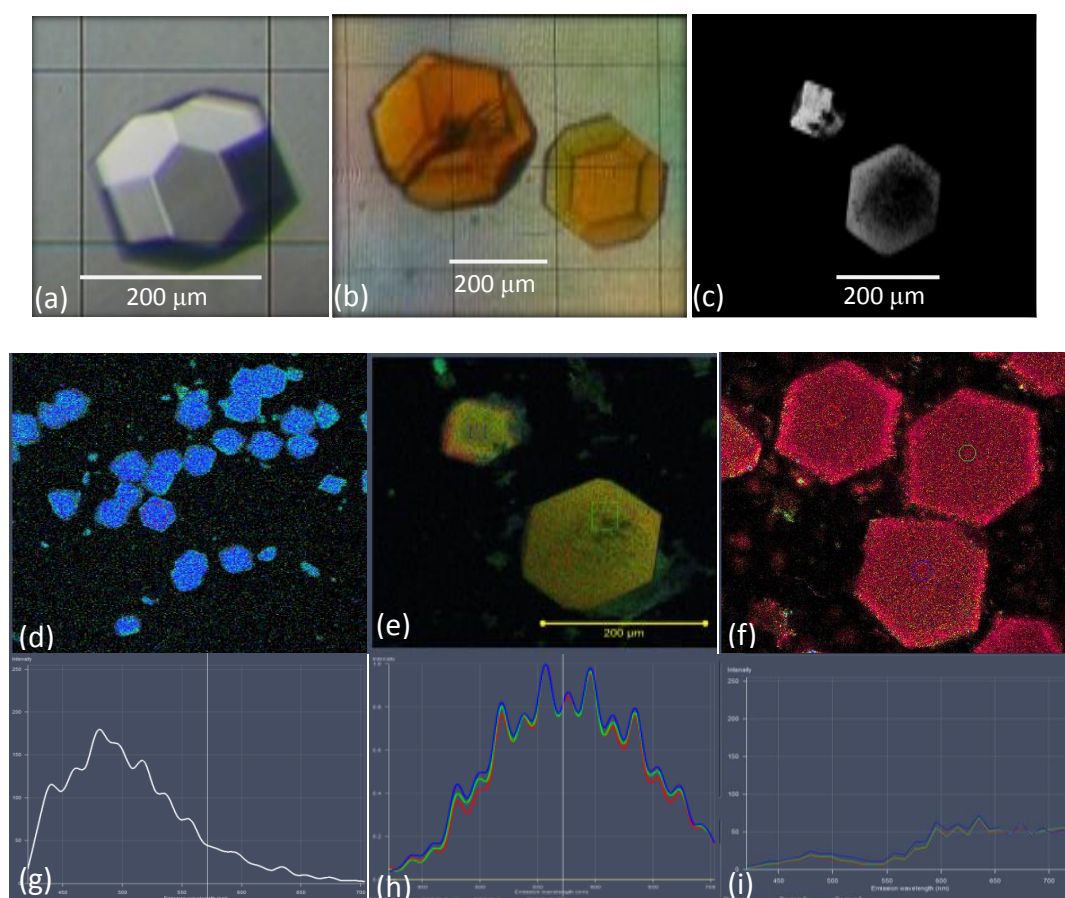

Fig. 3 Fluorescent images and spectra of insulin crystals and insulin-Au crystals.

(a) Image of insulin crystal

(b) Image of insulin-Au crystals

(c) 3D image of insulin-Au crystals

(d) Fluorescent insulin crystals image.

(e) Fluorescent insulin-Au crystals image.

(f) Fluorescent insulin-Au crystals image after 12hr.

(g) Fluorescent spectrum of insulin crystals (λ_{max}= 490 nm).

(h) Fluorescent spectrum of insulin-Au crystals (λ_{ex}= 406 nm, λ_{max}= 575 nm)

(i) Fluorescent spectrum of insulin-Au crystals after 12 hr (λ_{ex}= 406 nm, λ_{max}= 670 nm).

DLS shows the mean size of insulin-Au nanodots is 3.5±0.4 nm [Fig. 4 (d)]. The particle size, mainly for gold nanodots, was calculated to be 0.92±0.03 nm, based on 100 particles in TEM image [Fig. 4 (1)].

The diameter of gold nanodots is 0.92±0.03 nm confirmed by TEM [Fig. 4 (a)] The binding energy measured by XPS proves the type of gold and the reduction in the synthesis because the Au $4f^{7/2}$ spectrum could be deconvoluted into two distinct components (red and blue curves) centered at binding energies of 84.0 and 85.1 eV, which could be assigned to Au(0) and Au(I), respectively (Au(0)-75.7%, Au(I)-24.3%] [Fig. 4 (b)]. There is an asymmetrical characteristic peak, which can be further decomposed into two peaks at 84.0 and 85.3 eV. These two peaks indicate the presence of Au (0) and Au (I), respectively. Similarly, the asymmetrical $Au^{5/2}$ is decomposed to the Au (0) (87.76 eV) and Au (I) (88.81 eV). The results are consistent with previous study of Au nanodots, concluding the existence of a small amount of Au (I) on the surface of Au nanodots to help stabilizing the Au nanodots.
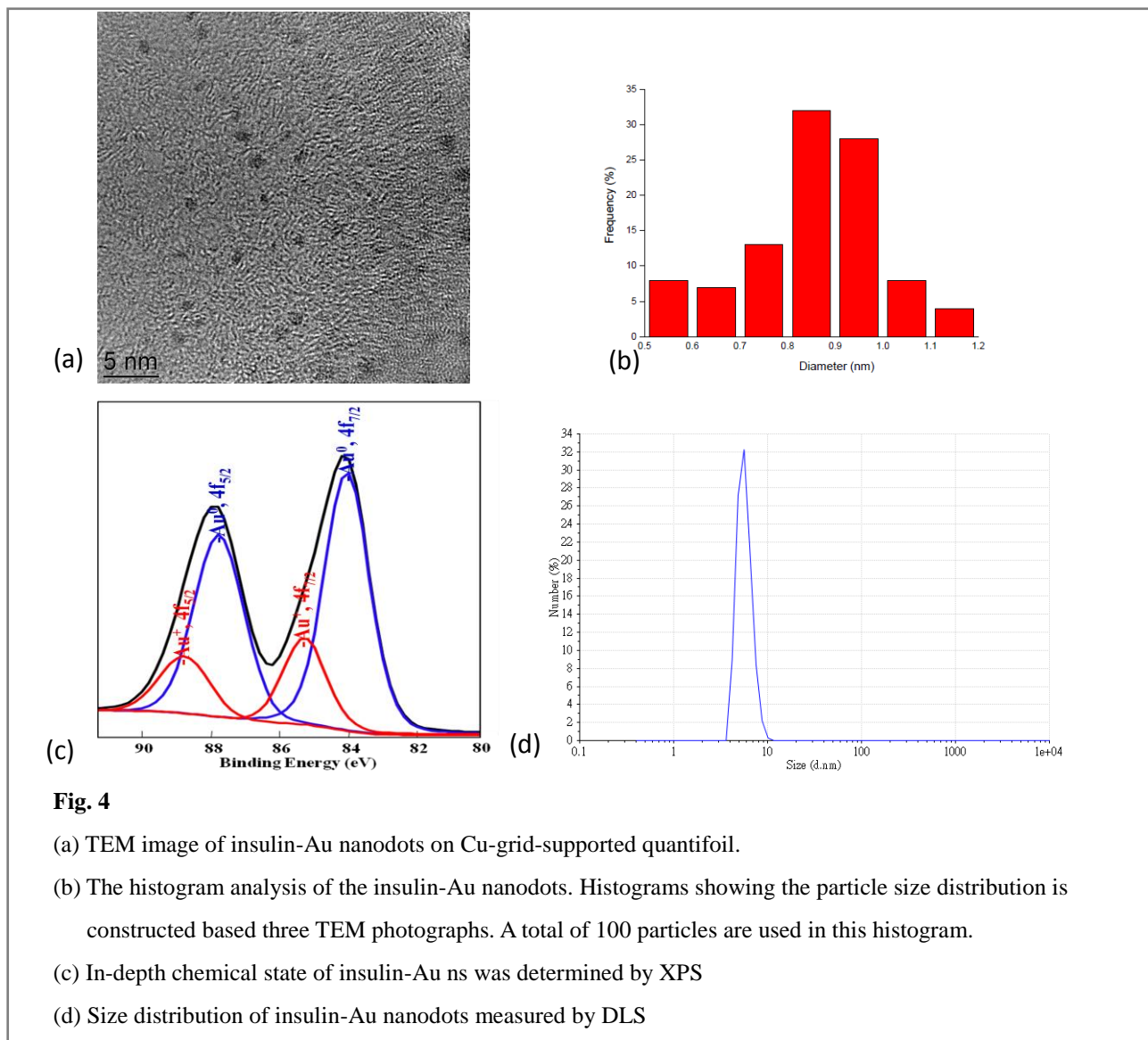

Fig. 4

(a) TEM image of insulin-Au nanodots on Cu-grid-supported quantifoil.

(b) The histogram analysis of the insulin-Au nanodots. Histograms showing the particle size distribution is constructed based three TEM photographs. A total of 100 particles are used in this histogram.

(c) In-depth chemical state of insulin-Au ns was determined by XPS

(d) Size distribution of insulin-Au nanodots measured by DLS

2. Biological activity of insulin-Au nanodots

(A) Cytotoxicity

      The results of MTT assay shows that insulin-Au nanodots have no significant cytotoxicity on C2C12 myoblast cells at 250 μg/mL insulin-Au nanodots [Fig. 5 (a)].

(B) Binding with receptors

      Z-stacking shows the insulin-Au nanodots was on the cell membrane and inside the cells, which indicates the receptor-mediate endocytosis [Fig. 5 (b)]. It preliminary implies that the red fluorescent insulin-Au nanodots remains the bioactivity of insulin.
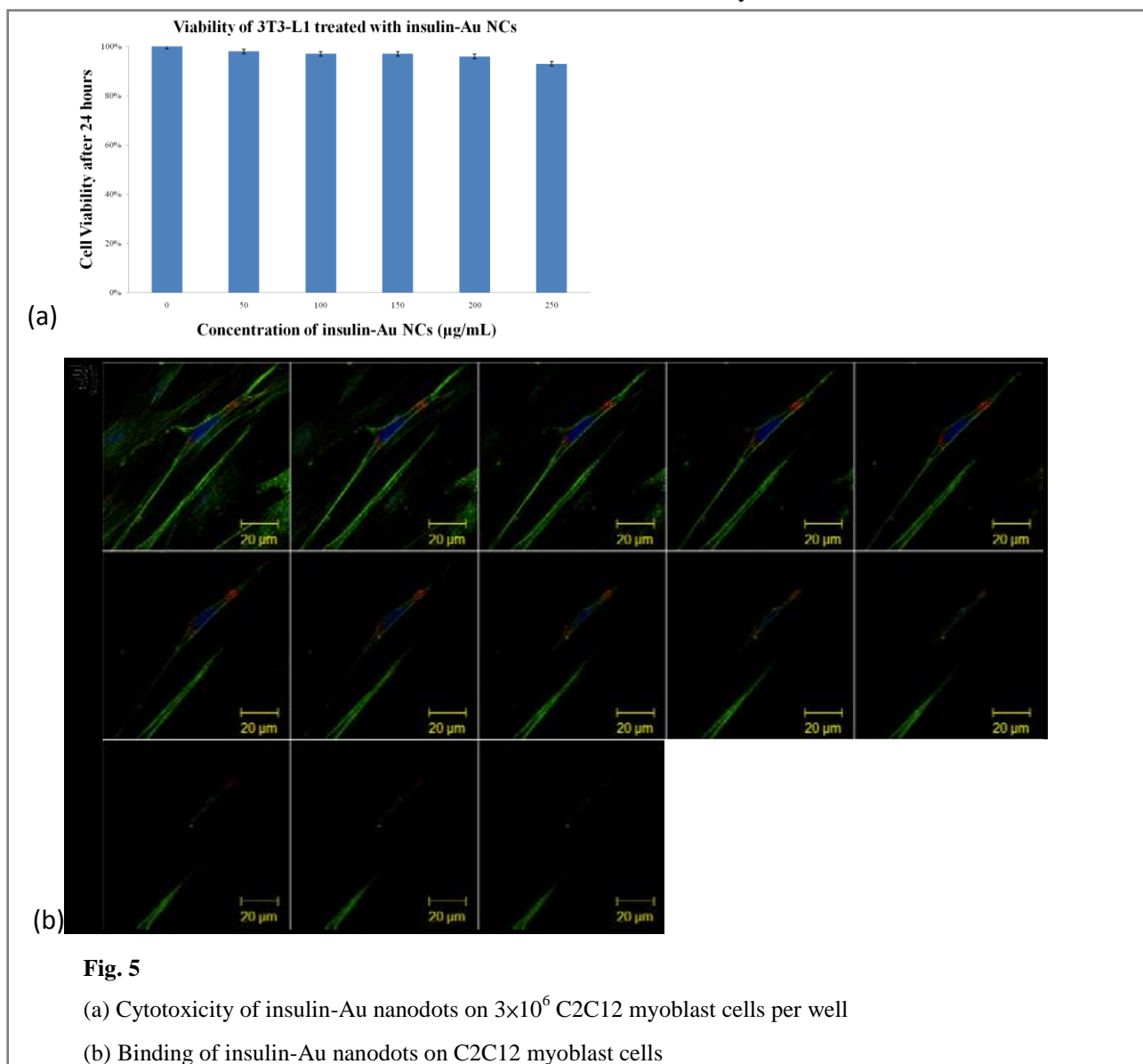

Fig. 5

(a) Cytotoxicity of insulin-Au nanodots on 3×10^6 C2C12 myoblast cells per well

(b) Binding of insulin-Au nanodots on C2C12 myoblast cells

(C) Glucose uptakes by cells

The glucose uptake promoted by insulin-Au nanodots is similar to that by insulin, which is 20% higher than that in vehicle control. [Fig. 5]. Since the biological activity of insulin is to stimulate the glucose uptake by binding to the specific receptors, the glucose uptake assay demonstrates that the insulin-Au nanodots maintain the biological activity of insulin. With the biological activity of insulin, we can trace insulin by the red fluorescence from insulin-Au nanodots *in vitro* or *in vivo*.
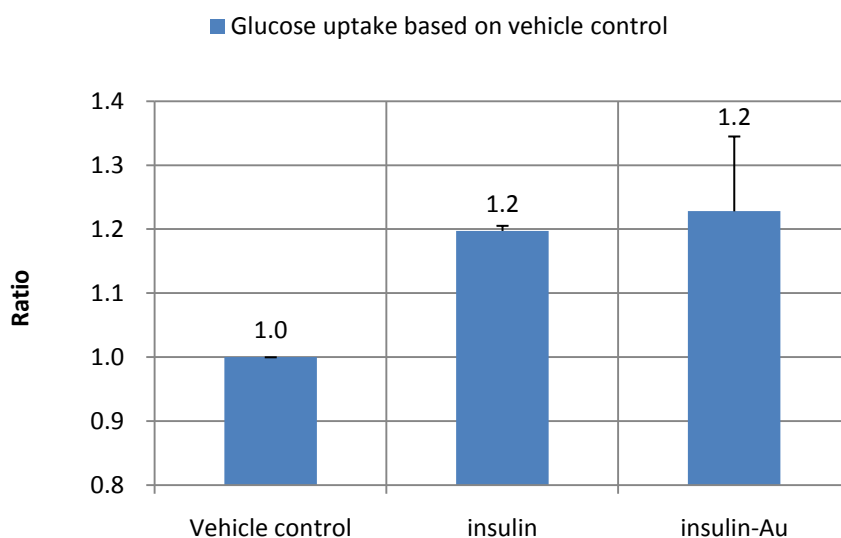
■ Glucose uptake based on vehicle control

Fig. 6 Glucose uptake assay of insulin and insulin-Au on 1×10^5 L6 rat skeletal muscle cells per well via absorption.

§ **Conclusions**

The red fluorescent insulin-Au nanodots are successfully synthesized by adding insulin 10 mg in $Na_3PO_{4(aq)}$ (0.1 M, pH 10.4, 800 μL) and $HAuCl_{4(aq)}$ (20 mg/mL, 200 μL) at 4°C for 12 hr.

The red fluorescent insulin-Au crystals are obtained, which could be used to define the insulin-Au structure.

With the low cytotoxicity, minute photobleaching and full biological activity of insulin, insulin-Au nanodots are promising biomarkers in vitro or in vivo. By tracing the red fluorescence of insulin-Au nanodots, we could have a better understanding of diabetes and Alzheimer's disease or even help the development of new drugs.

§ **References**

[1]   Alan R. Saltiel & C. Ronald Kahn, *Nature* **2001**, *414*, 799-806
[2]   Oleg Varnavski, Guda Ramakrishna, Junhyung Kim, Dongil Lee, and Theodore Goodson, *J. Am. Chem. Soc.* **2010**, *132*, 16-17
[3]   Jie Zheng, Philip R. Nicovich and Robert M. Dickson, *Annu. Rev. Phys. Chem.* **2007**, *58*, 409-431.
[4]   Christof M. Niemeyer, *Angew. Chem. Int. Ed.* **2001**, *40,* 4128-4158
[5]   Jianping Xie, Yuangang Zheng, and Jackie Y. Ying, *J. Am. Chem. Soc.* **2009**, *131*, 888-889